

6-24-1994

Meson-meson scattering in 2+1 dimensional lattice quantum electrodynamics

Alberto Luis Domínguez
Florida International University

DOI: 10.25148/etd.FI15101213

Follow this and additional works at: <https://digitalcommons.fiu.edu/etd>

 Part of the [Physics Commons](#)

Recommended Citation

Domínguez, Alberto Luis, "Meson-meson scattering in 2+1 dimensional lattice quantum electrodynamics" (1994). *FIU Electronic Theses and Dissertations*. 3076.

<https://digitalcommons.fiu.edu/etd/3076>

This work is brought to you for free and open access by the University Graduate School at FIU Digital Commons. It has been accepted for inclusion in FIU Electronic Theses and Dissertations by an authorized administrator of FIU Digital Commons. For more information, please contact dcc@fiu.edu.

FLORIDA INTERNATIONAL UNIVERSITY

Miami, Florida

**MESON-MESON SCATTERING
IN 2+1 DIMENSIONAL LATTICE
QUANTUM ELECTRODYNAMICS**

A thesis submitted in partial satisfaction of the

requirements for the degree of

MASTER OF SCIENCE

IN

PHYSICS

by

Alberto Luis Domínguez

1994

To: Dean Arthur W. Herriott
College of Arts and Sciences

This thesis, written by Alberto Luis Domínguez, and entitled Meson-Meson Scattering in 2+1 Dimensional Lattice Quantum Electrodynamics, having been approved in respect to style and intellectual content, is referred to you for judgement.

We have read this thesis and recommend that it be approved.

Mark Leckband

Xuewen Wang

Stephan L. Mintz

H. Rudolf Fiebig, Major Professor

Date of Defense: June 24, 1994

The thesis of Alberto Luis Domínguez is approved.

Dean Arthur W. Herriott
College of Arts and Sciences

Dr. Richard L. Campbell
Dean of Graduate Studies

Florida International University, 1994

© COPYRIGHT 1994 by Alberto Luis Domínguez

All rights reserved

DEDICATION

This thesis is dedicated to my mother, without whose financial assistance and emotional support it could never have been written.

ACKNOWLEDGEMENTS

I wish to thank all the members of my committee for their help and patience during the completion of this thesis. Their comments and suggestions have resulted in a much clearer presentation of my work. Thanks are also due to the friends who read rough drafts of this work. Many of their comments and suggestions have also been incorporated into this final draft. Needless to say, any remaining shortcomings are entirely my own responsibility.

I wish to take this opportunity to thank especially Professor Rudolf Fiebig for his instruction, assistance and friendship over the last seven years. Without his unwavering support and constant encouragement during my graduate work, it would not have been possible for me to complete this thesis and finish my degree.

I also wish to acknowledge the paper "Meson-Meson Scattering in 2+1 Dimensional Lattice Quantum Electrodynamics" by H. R. Fiebig, R. M. Woloshyn and A. L. Domínguez, published in Nuclear Physics B (1994) 418, 637, from which the present work draws heavily.

ABSTRACT OF THE THESIS

MESON-MESON SCATTERING IN 2+1 DIMENSIONAL LATTICE QUANTUM ELECTRODYNAMICS

by

Alberto Luis Domínguez

Florida International University, 1994

Professor H. Rudolf Fiebig, Major Professor

For three-dimensional compact lattice quantum electrodynamics, the meson-meson energy spectrum is obtained from a truncated time-correlation matrix of field operators. The energy levels indicate a slightly attractive residual interaction between the mesons. From the finite-volume spectrum, the scattering phase shifts can be calculated for the various irreducible representations of the lattice symmetry group. The s-wave phase shifts indicate short-range repulsion, while the d-wave data indicate intermediate-range attraction. This work serves as a model for describing the strong nuclear force from basic principles.

TABLE OF CONTENTS

List of Figures and Tables.....	viii
I. Introduction	
1. Organization of this Thesis.....	1
2. The "Standard Model" of Particle Physics.....	2
3. Work on Earlier Related Problems.....	4
4. Earlier Work on the Present Problem	
i. 1+1-Dim. Non-Relativistic Quantum Mechanics.....	6
ii. 1+1-Dim. Quantum Field Theory.....	8
iii. 3+1-Dim. (and 2+1-Dim.) Quantum Field Theory.....	9
5. Our Solution Method.....	10
5. Proof of Equation I.1.....	11
6. Notes.....	12
II. Lattice Gauge Theory	
1. The Wilson Gauge Action.....	15
2. The Fermion Action.....	17
3. Notes.....	18
III. Correlation Functions	
1. Two-Point Correlation Functions.....	21
2. Four-Point Correlation Functions.....	24
3. Properties of the Four-Point Correlation Function.....	27
4. The Truncated Time-Correlation Matrix.....	28
5. Notes.....	28
IV. Numerical Results	
1. Random-Source Technique.....	31
2. Time-Correlation Functions.....	31
3. Our Choice of Parameters.....	32
4. The Lattice Simulation Procedure.....	34
5. The Numerical Results.....	35
6. Notes.....	37
V. Solutions to the Schrödinger Equation	
1. Lüscher's Model in Two Space Dimensions.....	50
2. Singular Periodic Solutions.....	51
3. Notes.....	53
VI. Extracting the Phase Shifts	
1. Partial Wave Analysis.....	55
2. The Phase Shift Condition.....	56
3. Notes.....	59
VII. Conclusion	
1. Explanation of Results.....	64
2. Consideration of Future Work.....	66
Appendix A	69
Appendix B	74
List of References.....	76

LIST OF FIGURES AND TABLES

Figure I.1	Illustration of Equation I.1.....	14
Figure II.1	Illustration of Equation II.1.....	20
Figure III.1	Illustration of Equation III.18.....	29
Figure III.2	Range of Momenta.....	30
Figure IV.1	Wilson Line versus Coupling Parameter.....	39
Figure IV.2	Illustration of Confinement-Deconfinement Phase Transitions.....	40
Figure IV.3	Mesonic Mass versus L	41
Figure IV.4	Contributions to C' in A_1 and A_2	42
Figure IV.5	Contributions to C' in B_1 and B_2	43
Figure IV.6	Illustration of Equation IV.5.....	44
Figure IV.7	Eigenvalues in A_1	45
Figure IV.8	Eigenvalues in A_2	46
Figure IV.9	Eigenvalues in B_1	47
Figure IV.10	Eigenvalues in B_2	48
Table I	Least-Squares Fit to $C^{(2)}(t, t_0)^2$	49
Table II	Phase Shifts $\delta_1^{(\Gamma)}(k_n^2)$	60
Figure VI.1	Phase Shifts for Partial Wave $l=0$	61
Figure VI.2	Phase Shifts for Partial Wave $l=2$	62
Figure VI.1	Phase Shifts for Partial Wave $l=4$	63
Figure VII.1	Typical $l=0$ Scattering Wave.....	67
Figure VII.2	Typical $l=2$ Scattering Wave.....	68

I. INTRODUCTION

1. Organization of this Thesis

This thesis uses a lattice gauge theory numerical simulation to calculate the scattering phase shifts of two mesons scattering off each other and attempts to interpret these phase shifts in a manner consistent with nuclear physics experimental data. This work could serve as a foundation for a fundamental explanation of the strong nuclear force in terms of gauge fields.

The work involved in this thesis divides naturally into two parts. The first part involves the analytic calculation of the four-point correlation functions. These correlation functions are then used to obtain the two-body energy spectrum, from which we can then extract the corresponding discrete set of values of the momentum. The second part involves the numerical calculation of the energy-dependent M-matrix, which is in turn used to solve numerically the determinant condition for the scattering phase shifts $\delta(k)$.

This manuscript is divided into seven chapters. The present Chapter I provides a historical and theoretical introduction to this field of research, a discussion of earlier work on our problem and related problems, a brief explanation of the "standard model" of elementary particle physics, and an overview of our solution method. Chapter II gives a brief review of the relevant lattice gauge theory and an explanation of the fermion matrix and its inverse. Chapter III explains the analytic derivation of the two-point and four-point time correlation functions, which is the endpoint of the analytical aspect of this work. Chapter IV provides an overview of how the two-body energy spectrum and the corresponding values

of the momentum are calculated, discusses some of the computational difficulties, explains the numerical procedures and parameters used in this work, and uses the four-point correlation function to obtain the momenta. Chapter V gives the solution of the Schrödinger equation for our problem, and derives the M-matrix from these solutions. Chapter VI explains the method for solving the determinant condition, gives a partial wave analysis of our problem, extracts from this partial wave analysis the scattering phase shifts, and gives graphs of the scattering phase shifts as a function of the momentum squared, which is the final goal of this work. Chapter VII gives a brief explanation of our numerical results, considers directions in which this work might lead future research, and discusses how this work could lead to an explanation of the strong nuclear force from basic principles. Each chapter finishes with its own set of endnotes and a discussion of other work which should be read in conjunction with that chapter.

2. The "Standard Model" of Particle Physics

Physicists presently believe that there are four basic forces in nature: the electromagnetic force (responsible for the binding of nuclei and electrons into atoms and the binding of atoms into molecules), the strong nuclear force (responsible for the binding of protons and neutrons into complex nuclei and the confinement of quarks into mesons and hadrons), the weak nuclear force (responsible for beta decay of nuclei and neutrons and the decay of the muon), and the gravitational force (responsible for the motion of planets and galaxies and the large-scale structure of the universe). Presently, gravity is explained by Einstein's theory of general relativity, and the other three forces are described by the

"standard model" of particle physics.

The standard model consists of the electroweak theory and quantum chromodynamics. The electroweak theory was developed between 1961 and 1968 by Sheldon Glashow, Abdus Salam and Steven Weinberg. To understand how the theory was developed, we must first discuss quantum electrodynamics, developed by Richard Feynmann, Julian Schwinger and Shinichero Tomonaga in the 1940s. The invariance of the equations of quantum electrodynamics under certain transformations of the electromagnetic field (called gauge transformations) led to the formulation of the theory as a gauge field theory where the photon is the gauge (interaction) field mediating the electromagnetic force. In quantum electrodynamics, the gauge fields are subject to the gauge symmetry group $U(1)$, the unitary group in 1 dimension. Glashow, Salam and Weinberg independently discovered that the electromagnetic and weak forces could be described by a single theory which contained the photon as a gauge field, but also contained gauge fields capable of explaining the weak nuclear force. Their electroweak, or GSW, theory predicted the W^\pm and Z^0 bosons as the gauge fields mediating the weak force. These gauge fields were subject to the gauge symmetry group $SU(2)$, the special unitary group of 2×2 matrices. The electroweak theory was verified when the W^\pm and Z^0 were discovered at CERN in 1983. This theory unified the electromagnetic and weak forces by showing them to be different manifestations of the same interaction, which was subject to the gauge symmetry group $SU(2) \otimes U(1)$.

The foundation for quantum chromodynamics was laid by Murray Gell-Mann and Yuval Neeman in 1961 when they proposed a grouping scheme for particles which interacted via the strong nuclear force. Their grouping scheme was subject to the symmetry group

$SU(3)$, the special unitary group of 3×3 matrices. Soon thereafter, Gell-Mann and Zweig proposed the existence of quarks as the elementary building blocks of mesons and hadrons. In the 1960s and 1970s, it came to be known that the grouping scheme of Gell-Mann strong nuclear force could be explained using a gauge field theory in which the gauge fields are subject to the gauge symmetry group $SU(3)$, the same group as in Gell-Mann's earlier theory. This theory is quantum chromodynamics (QCD), in which quarks are the fundamental particles, which interact through gauge fields called gluons. In QCD, mesons and hadrons are no longer found to be fundamental, as was believed until the 1960s. The present theory states that mesons are made up of a quark-antiquark pair and hadrons are made up of three quarks.

Many physicists believe that there should be a single "grand unified" gauge field theory which contains the gauge fields of both the electroweak theory and QCD and unifies all three forces (electromagnetic, weak and strong), showing them to be different aspects of the same theory. The gauge symmetry group of such a theory would have to contain $SU(3) \otimes SU(2) \otimes U(1)$. Until recently, the most popular candidate for a "grand unified theory" was based on the gauge symmetry group $SU(5)$. However, to date, no "grand unified theory" has made successful predictions.

3. Work on Earlier Related Problems

In particle physics, the standard model consisting of the electroweak theory and QCD is generally believed to explain all fundamental physics at all presently accessible energies. However, it has so far proved impossible to compare the experimental data for low-energy

hadron-hadron scattering with the theoretical predictions of QCD, because the latter are very difficult to obtain.

One of the most promising attempts to solve QCD at the low energies relevant to nuclear physics is lattice gauge theory, introduced by Wilson in 1974. In Wilson's lattice formulation of gauge theory, the fields are placed on a discrete Euclidean spacetime lattice and the functional integral is computed by numerical simulation. This formulation is a non-perturbative approach to gauge field theories. It involves approximating the continuous spacetime of traditional quantum field theory (which provides the formalism on which all gauge field theories are based) with a Euclidean lattice. This seems a very natural way of regulating the ultraviolet divergences endemic to quantum field theory. Since no two points can ever be closer than the lattice spacing a , the maximum momentum Λ correspondingly is of the order \hbar/a . Therefore, Wilson's lattice formulation of gauge field theory contains a natural ultraviolet cutoff.

Wilson's work was based on the concept of a gauge field as a path-dependent phase factor². In Wilson's formulation we associate an independent element U_{ij} of the given gauge group G with each link between two nearest-neighbor lattice sites i and j . In the present text, the additional indices arising from the fact that the U_{ij} may be matrices (as in the cases of $SU(2) \otimes U(1)$ and $SU(3)$) are suppressed. The mathematical details of Wilson's lattice gauge theory are contained in Chapter II.

Wilson's lattice formulation of QCD has been extensively used to obtain hadron masses. Furthermore, since the energy of a two-particle state on a finite-volume lattice differs from its energy $E_0=2m$ on an infinite-volume lattice by correction terms which

involve the scattering length³, the lattice formulation can also be used to calculate scattering lengths. This method has been successfully applied to the problem of obtaining π - π and π - N scattering lengths in lattice QCD₃₊₁⁴.

4. Earlier Work on the Present Problem

(i) 1+1 Dimensional Non-Relativistic Quantum Mechanics

The next logical step in the lattice formulation of QCD₃₊₁ would be to calculate scattering phase shifts. And, indeed, it is possible to calculate phase shifts using the finite-size effects of the lattice formulation, even though the procedure is significantly more complex than the one for calculating scattering lengths.

In one space dimension, the scattering phase shifts $\delta(k)$ for two non-relativistic point-like spinless bosons can be obtained from the equation⁵

$$e^{2i\delta(k)} = e^{-ikL} \tag{I.1}$$

where the relative momenta k can be extracted from the discrete finite-volume lattice energy spectrum in the relative coordinate

$$E = \frac{k^2}{m} \tag{I.2}$$

The formal derivation of equation I.1 has been relegated to section I.6 to preserve continuity. However, it seems useful at this point to consider a fairly intuitive physical interpretation of this equation.

For a given interaction potential $V(z)$ and box size L , the Schrödinger equation with periodic boundary conditions has a discrete set of solutions which then yields all the possible finite-volume energy levels, $E_n = k_n^2/m$ with $n \in \mathbb{N}$. This reminds us of the general result of quantum mechanics that a free particle can have any energy value while a bound particle (such as our particle in a box of length L) can have only certain discrete energy values. However, in addition to this obvious interpretation as a quantization condition on our system, there is a much more fundamental physical significance to this equation.

If we look at figure I.1a, we see that, in the non-interacting case, the wavefunction for the particle in the box smoothly connects to itself when the endpoints $z = \pm L/2$ are identified, which is reminiscent of the periodic boundary conditions discussed above. But the introduction of an interaction $V(z)$ distorts the wavefunction in the interaction region around $z=0$ in such a way that the asymptotically free waves near the endpoints, $z = \pm L/2$, are phase shifted relative to each other by $2\delta(k)$. This is illustrated in figure I.1b for the case of an attractive potential. Looking at figure I.1c, we see that the periodicity can be restored by changing either k or L until the equation $2\delta(k) = kL \pmod{2\pi}$ is satisfied.

So equation I.1 tells us that the kinematical phase shift which one picks up when translating a free wave of momentum k by a distance L and the phase shift which results from the scattering of the particles must exactly compensate each other to guarantee the periodicity of the wave.

(ii) 1+1-Dimensional Quantum Field Theory

In a relativistic quantum field theory in one space dimension, equation I.1 remains

the same and the relative momenta k can still be extracted from the discrete energy spectrum, which is now given by

$$E = 2 \sqrt{m^2 + k^2} \quad (\text{I.3})$$

The interpretation of the scattering phase shift equation in a relativistic quantum field theory is the same as the one discussed above for non-relativistic quantum mechanics. The phase $\delta(x)$ by which a free-particle state of momentum k transforms under translations over a distance L is $kL/2$. The only difference comes in the energy-momentum equation. It is worth noting that, in the case of quantum field theory, equation I.1 can also be derived within the framework of the usual Feynman diagram expansion⁶. As a final comment, we note the restrictions on the applicability of equation I.1. The equation is expected to hold in any 1+1 dimensional quantum field theory with only massive particles provided that

- (1) the finite-volume two-particle states are such that mixing with other many-particle states is suppressed,
- (2) L is larger than the interaction range so that the wavefunction is free for relative separations close to $z=\pm L/2$,
- (3) L is sufficiently large to avoid polarization effects from virtual particles interacting "around-the-world" across what is actually a relative separation close to $z=\pm L$ (an effect which is automatically negligible once condition 2 is satisfied), and
- (4) the lattice spacing is sufficiently small so that the Euclidean lattice correction terms (which vanish as a power of the lattice spacing) can be ignored.⁷

(iii) 3+1-Dimensional (and 2+1-Dimensional) Quantum Field Theory

In a relativistic quantum field theory in three space dimensions, equation I.3 remains valid, but the equation for obtaining $\delta(k)$ is more complicated,⁸

$$\det (e^{2i\delta(k)} - U(k)) = 0 \quad (\text{I.4})$$

where the matrix U is a shorthand notation,

$$U = (M+i)^{-1}(M-i) \quad (\text{I.5})$$

where $M=M(q^2)$, with $q=kL/2\pi$, is an energy-dependent matrix which emerges from constructing a Green's function for a short-ranged periodic potential⁹. The matrix M is a finite linear combination of the zeta functions defined by¹⁰

$$\zeta_{lm}(1;q^2) = \sum_{\vec{n}} y_{lm}(\vec{n}) \frac{1}{\vec{n}^2 - q^2} \quad (\text{I.6})$$

where

$$y_{lm}(\vec{r}) = r^l Y_{lm}(\theta, \varphi) \quad (\text{I.7})$$

are harmonic polynomials. The derivations of the energy-dependent M -matrix and the determinant condition I.4 on the scattering phase shifts are discussed at greater length in Chapters V and VI.

5. Our Solution Method

There are two fundamental difficulties involved in applying the procedure outlined above to the calculation of scattering amplitudes. The first complication is that, in order to obtain the four-point time correlation functions from a lattice simulation, the entire fermion propagator matrix must be calculated. We dealt with this complication by using several simplifying symmetries which reduced the need for numerical computation. This solution to the first complication is discussed at length in Chapter III. A second, even more serious, complication is that, due to computational limitations, the lattices which have been used so far are too small to contain two well-separated (slowly-moving) composite particles appropriate to the problem.

In our work, we sought to circumvent this second computational limitation by obtaining scattering data from a lattice simulation of QED_{2+1} rather than of QCD_{3+1} . Our choice of QED_{2+1} is easier to deal with numerically because of its lower dimensionality (two space dimensions instead of three) and the one-dimensional parameter space and Abelian structure of its $U(1)$ gauge group (as opposed to the larger parameter space and non-Abelian structure of the $SU(3)$ gauge group of QCD). But, despite its greater simplicity, QED_{2+1} shares several phenomenological characteristics with QCD_{3+1} , such as a confinement-deconfinement phase transition¹¹, spontaneous chiral symmetry breaking¹², and the existence of composite mesonic (i.e. fermion-antifermion) particle states¹³.

For these reasons, we used the QED_{2+1} model to learn about the interactions of two composite mesonic particles in the hope that the results might be suggestive of the behavior of the physically significant QCD_{3+1} model. Also, we hoped that we could use our work to

learn about the usefulness and limitations of certain numerical techniques.

6. Derivation of Equation I.1

Consider two identical spinless pointlike bosons moving on a line in one space dimension. The Schrödinger wavefunction $\psi(x,y)$ depends on the positions x and y of the two particles and must be symmetric under the interchange of x and y . If we furthermore restrict ourselves to states with zero total momentum, then we have the condition $\psi(x,y)=f(x-y)$, where $f(z)=f(-z)$.

The stationary Schrödinger equation in infinite volume reduces to

$$\left[-\frac{1}{m} \frac{d^2}{dz^2} + V(|x|) \right] f(z) = Ef(z) \quad (\text{I.8})$$

Since $f(z)$ must be even, there is only one admissible linearly independent solution for any given energy value E , which we will indicate by $f_E(z)$. If $E=k^2/m$ with $k \geq 0$, then $f_E(z)$ is a stationary scattering solution, which can be normalized so that

$$f_E(z) = \cos(k|z| + \delta(k)) = 0 \quad \text{in the limit } |k| \rightarrow \infty \quad (\text{I.9})$$

Now suppose that the particles are enclosed in a periodic box of length L , so that we must take into account "around-the-world" effects. Then the stationary Schrödinger equation becomes

$$\left[-\frac{1}{m^2} \frac{d^2}{dz^2} + \sum_{v \in Z} V(|z+vL|) \right] f(z) = Ef(z) \quad (\text{I.10})$$

The periodicity condition implies that $f_E'(-L/2) = f_E'(L/2) = 0$. Recalling the limit

I.9, we conclude that

$$kL + 2\delta(k) = 0 \pmod{2\pi} \tag{I.11}$$

which can be restated as

$$e^{2i\delta(k)} = e^{-ikL}$$

which is equation I.1.

7. Notes

A discussion of the standard model can be found in Cooper & West (1988) and Hughes (1985) at a fairly elementary level, in Aitchison & Hey (1989) at an intermediate level, and in Renton (1990) and Cheng & Li (1984) at a fairly sophisticated level. Fiebig, Woloshyn and Domínguez (1994) contains an excellent summary of previous work in this field. Lüscher (1986) and Lüscher and Wolff (1990) are the sources for equation I.1. Lüscher (1991a) and Lüscher (1991a) are the sources for equation I.4.

1. Wilson (1974).
2. Creutz (1983), chapter 7.
3. Hamber et al (1983).
4. Guagnelli, Marinari and Parisi (1990).
Sharpe (1991).
Sharpe, Gupta and Kilcup (1992).
5. Lüscher (1986).
Lüscher and Wolff (1990).
6. Lüscher (1986).

7. Lüscher and Wolff (1990).
8. Taylor (1983), chapter 11.
9. Fiebig, Woloshyn and Domínguez (1994).
10. Lüscher (1991a).
Lüscher (1991b).
Fiebig, Woloshyn and Domínguez (1994).
11. Coddington et al (1986).
12. Dagotto, Kogut and Kocic (1989).
Barbour et al (1984).
13. Kogut and Susskind (1975).
Susskind (1977).

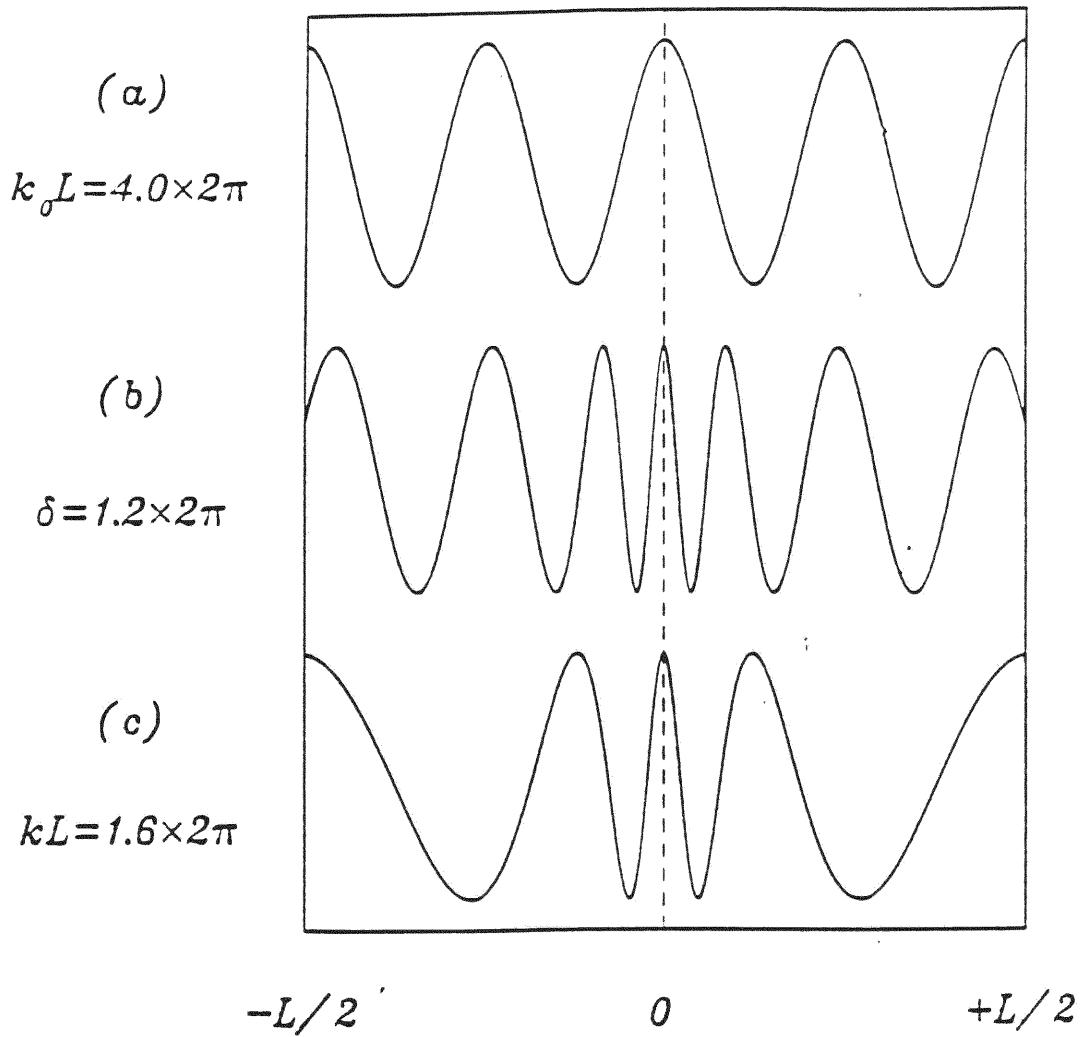


FIGURE I.1
 ILLUSTRATION OF EQUATION I.1

Generic solutions $\psi(x)$ of the Schrödinger equation
 (a) with no interaction,
 (b) with an attractive potential around $x \approx 0$, and
 (c) with decreased wave number k to restore the original phase condition.

II. LATTICE GAUGE THEORY

1. The Wilson Gauge Action

The first step of Wilson's lattice formulation of gauge field theory is to define an appropriate gauge action for the theory. We will consider a few obvious requirements for this action before we attempt to write down a naïve expression for it. The action, which will be composed only of the link variables U_{ij} defined above, should be real and bounded, should be gauge invariant and should reduce to the continuum action as $a \rightarrow 0$.

The simplest gauge-invariant combination of link variables consists of four link variables which form a closed loop, called a plaquette¹. Hence, we choose our expression for the lattice plaquette action by taking the path-dependent product of the link variables U_{ij} around the plaquette, which actually does possess all of the above properties. Our notation for this plaquette is

$$U_{\mu\nu}(x) = U_{\nu}^{+}(x)U_{\mu}^{+}(x+a_{\nu})U_{\nu}(x+a_{\mu})U_{\mu}(x) \quad (\text{II.1})$$

The reason for this notation will best be appreciated by looking at figure II.1.

The plaquette action is then given by

$$S_{\square}[U] = \beta \left[1 - \frac{1}{N} \Re(\text{Tr}(U_{\mu\nu}(x))) \right] \quad (\text{II.2})$$

where N is the dimension of the gauge group square matrices, and the constant β will be determined later. Tr and \Re mean that we take first the trace of the matrix $U_{\mu\nu}$ and then the real part of this trace. The total Wilson action is then given by the appropriate sum over all

plaquettes.

$$S = \sum_{\square} S_{\square}[U] \quad (\text{II.3})$$

Hereafter, we will limit our discussion to the gauge group of quantum electrodynamics, U(1), in order to obtain the specific results needed for our simulation of QED₂₊₁. For the U(1) gauge theory, the link variables are given by

$$U_{\mu}(x) = e^{igA_{\mu}(x)} \quad (\text{II.4})$$

where $A_{\mu}(x)$ is an angle, $0 \leq A_{\mu}(x) < 2\pi/g$, and g is the coupling constant.

Now we need to work through the algebra resulting from the substitution of equation II.4 into equation II.1. Aided by the fact that all the link variables commute, we arrive at

$$U_{\mu\nu}(x) \rightarrow e^{iga^2[\partial_{\nu}A_{\mu} - \partial_{\mu}A_{\nu}]} \quad (\text{II.5})$$

in the limit $a \rightarrow 0$.

In the U(1) case, the plaquette action II.2 is given by

$$S_{\square}[U] = \beta[1 - \Re(U_{\mu\nu}(x))] \quad (\text{II.6})$$

which, in the limit $a \rightarrow 0$, simplifies to

$$S_{\square}[U] = \frac{\beta g^2 a^4}{2} F_{\mu\nu}^2 \quad (\text{II.7})$$

where $F_{\mu\nu} = \partial_{\mu}A_{\nu} - \partial_{\nu}A_{\mu}$ is the usual field strength tensor².

Two things about this action are worth noting. First, we note that, in the continuum limit $\Sigma_x a^4 \rightarrow \int d^4x$, the total Wilson action simplifies to the usual continuum result if we identify the constant β with $1/2g^2$.

$$S[U] = \int d^4x \frac{1}{4} F_{\mu\nu}^2 \quad (\text{II.8})$$

Second, we note that the Wilson action II.7 is gauge invariant, as must be demanded.

2. The Kogut-Susskind Fermion Action

Fermion (matter) fields can now be introduced in two ways, using Wilson fermions³ or using Kogut-Susskind (staggered) fermions⁴. In either case, the fermion action is written

$$S_F[U, \bar{\chi}, \chi] = \sum_{x,y} \bar{\chi}_f(x) G_{x,y}^{-1}[U] \chi_f(y) \quad (\text{II.9})$$

where $f=u,d$ are the flavours of the fermion field, "up" and "down", and the sum extends over all lattice sites x,y . The fermions fields, χ and $\bar{\chi}$, are one-component Grassmann fields which live on the lattice sites, in contrast to the gauge fields U_{ij} , which live on the lattice links.

In the case of staggered fermions, the Dirac operator or fermion matrix, $G_{x,y}^{-1}[U]$ is⁵

$$G_{x,y}^{-1} = \frac{1}{2} a^3 \sum_{\mu} \eta_{\mu}(x) [U_{\mu}(x) \delta_{x+\mu,y} - U_{\mu}^{\dagger}(y) \delta_{x,y+\mu}] + a^4 m_F \delta_{x,y} \quad (\text{II.10})$$

where $\eta_{\mu}(x)$ is the staggered phase (± 1) and m_F is the bare fermion mass.

The partition function, written as a path integral, is

$$Z = \int [dU][d\chi][d\bar{\chi}] e^{-S_B[U]} e^{-S_F[U,\chi,\bar{\chi}]} \quad (\text{II.11})$$

where dU denotes the measure for the gauge group integration.

The integration over the Grassmann fields is Gaussian and can be carried out, with the simplified result⁶

$$Z = \int [dU] e^{-S_B[U] + \ln \det G} \quad (\text{II.12})$$

It is this last form of the partition function which is (in principle) amenable to numerical (Monte Carlo) simulation.

3. Notes

Much of the background for this chapter can be found in Creutz (1983), where the relevant lattice gauge theory is presented. The seminal paper on lattice field theory is Wilson (1974). The concepts of Wick rotation and Euclidean spacetime are central to the formulation of lattice gauge theories. These concepts are presented in Fetter & Walecka (1971), from an analytic point of view, and in Creutz (1983) and Ramond (1989), in a more modern formulation for numerical work. Kogut (1979), although written from the point of view of spin systems, is a very thorough review article. Kawamoto and Smit (1981) and Kluberg-Stern et al (1983) provide much information on Kogut-Susskind fermions. Burden and Burkitt (1987) considers lattice fermions in 2+1 dimensions.

1. Cheng & Li (1984), Sections 8.2 and 10.5.

2. Jackson (1975), chapter 11.
3. Wilson (1974).
Fiebig, Woloshyn and Domínguez (1994).
4. Kogut and Susskind (1975).
Susskind (1977).
Fiebig, Woloshyn and Domínguez (1994).
Kluberg-Stern et al (1983).
Kawamoto and Smit (1981).
5. Creutz (1983), chapter 5.
Cheng & Li (1984), Section 10.5.
Kawamoto and Smit (1981).
6. Ramond (1989), page 215.
Creutz (1983), chapter 5.

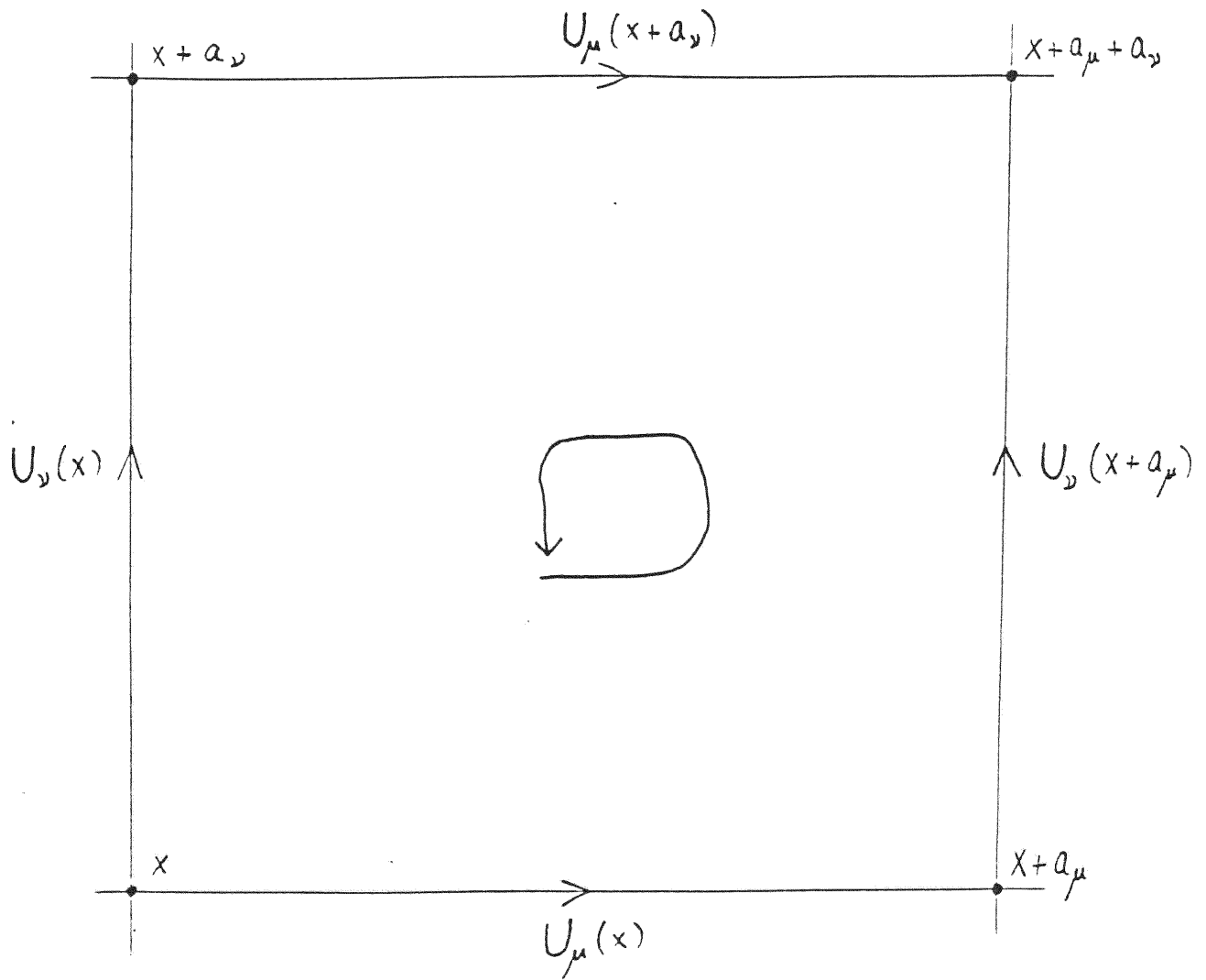


FIGURE II.1
 ILLUSTRATION OF EQUATION II.1

III. CORRELATION FUNCTIONS

1. Two-Point Correlation Function

As a preliminary to obtaining the meson-meson time-correlation matrix, we need to obtain the two-point correlation function. And, as a first step towards this goal, the mesonic operators are defined by

$$\phi_{\vec{p}}(t) = L^{-2} \sum_{\vec{x}} e^{i\vec{p}\cdot\vec{x}} \bar{\chi}_u(\vec{x}t) \chi_d(\vec{x}t) \quad \text{with } \vec{p} = \frac{2\pi}{L}(n_1, n_2) \quad (\text{III.1})$$

where the sum runs over the L^2 sites of the space lattice, and, as before, u and d are the flavours of the fermion fields, χ and $\bar{\chi}$, which represent a quark and an antiquark, respectively.

The two-point correlation function at zero momentum is given by

$$C^2(t, t_0) = \langle \phi_{\vec{0}}^+(t) \phi_{\vec{0}}(t_0) \rangle - \langle \phi_{\vec{0}}^+(t) \rangle \langle \phi_{\vec{0}}(t_0) \rangle \quad (\text{III.2})$$

The expectation value contains a product of four Grassman fields which can be expressed in terms of elements of the inverse fermion matrix G . Using a notation reminiscent of that used in Wick's Theorem, we define

$$G_2(x, y) = \langle : \bar{\chi}(x) \chi(y) : : \chi(x) \bar{\chi}(y) : \rangle_U \quad (\text{III.3})$$

where

$$: \bar{\chi}(x) \chi(y) : = G_{x,y}[U] \quad (\text{III.4})$$

is a contraction, and $\langle \rangle_U$ denotes averaging over all gauge field configurations with probability distribution $e^{-S_W[U]}$.

We then obtain for equation III.2 the expression

$$C^2(t, t_0) = L^{-4} \sum_{\vec{x}, \vec{y}} G_2(t\vec{x}, t_0\vec{y}) \quad (\text{III.5})$$

In general, we would now Fourier transform to momentum space because of the needs of the numerical aspects of the calculations. However, instead of the individual momenta, \mathbf{p}_1 and \mathbf{p}_2 , we will introduce the center-of-mass and relative momenta, \mathbf{P} and \mathbf{p} . This will yield the following expression for the correlation function.

$$C_{\vec{P}\vec{p}}^2(t, t_0) = L^{-4} \sum_{\vec{x}} \sum_{\vec{y}} e^{i\vec{P} \cdot \frac{1}{2}(\vec{x} + \vec{y})} e^{i\vec{p} \cdot (\vec{x} - \vec{y})} G_2(t\vec{x}, t_0\vec{y}) \quad (\text{III.6})$$

In particular, we will consider only those operators the center-of-mass momentum of which is zero.

$$C_{\vec{P}=0}^2(t, t_0) = L^{-4} \sum_{\vec{x}} \sum_{\vec{y}} e^{i\vec{p} \cdot (\vec{x} - \vec{y})} G_2(t\vec{x}, t_0\vec{y}) \quad (\text{III.7})$$

If we now took the relative momentum to be zero as well, the two-point time-correlation function would become

$$C_{\vec{P}=0}^2(t, t_0) = L^{-4} \sum_{\vec{x}, \vec{y}} G_2(t\vec{x}, t_0\vec{y}) \quad (\text{III.8})$$

which is identical to equation III.5.

There is an additional simplification to this equation which is allowed by the translational invariance of the system.

$$C_{\vec{p}=0}^2 = L^{-2} \sum_{\vec{x}} G_2(t\vec{x}, t_0\vec{0}) \quad (\text{III.9})$$

This form of the two-point time-correlation function is the one most widely used for hadron mass calculations because to employ it numerically one needs to calculate just one column of the inverse fermion matrix $G_{x,y}$. We, however, will not use this simplification because no such simplification seems to apply to the calculation of the time-correlation matrix of the two-meson system¹.

Inserting our earlier result III.5 into our form of the two-point time-correlation function III.8, we obtain

$$C_{\vec{p}=0}^2 = L^{-4} \sum_{\vec{x}} \sum_{\vec{y}} (G_{t\vec{x}, t_0\vec{y}})(G_{t\vec{x}, t_0\vec{y}})^* \quad (\text{III.10})$$

When the calculation is carried out with a large enough time axis (we used $L_t=32$), we obtain the asymptotic result for the square of the two-point time-correlation function.

$$C_{\vec{p}=0}^{(2)}(t, t_0)^2 \propto \cosh m(t-t_c) \quad (\text{III.11})$$

Since periodic boundary conditions are employed, the square of the two-point time-correlation function is symmetric about the center of the time axis. This is reflected in equation III.11 by the fact that $t_c = \frac{1}{2}L_t + 1 = 17$. The meson rest mass m can then be extracted from the asymptotic behavior of the time-correlation function around $t \approx t_c = 17$.

2. Four-Point Correlation Functions

In an analogous manner, we will now obtain the four-point time-correlation function.

We start in the same way by writing the mesonic four-point correlation function.

$$G_4(x_1, x_2, y_1, y_2) = \langle \phi^+(y_2) \phi^+(x_2) \phi(x_1) \phi(y_1) \rangle - \langle \phi^+(y_2) \phi^+(x_2) \rangle \langle \phi(x_1) \phi(y_1) \rangle \quad (\text{III.12})$$

There is a much more natural way of writing this expression. Let us introduce the meson-meson field operators.

$$\Phi_{\bar{p}}(t) = \phi_{-\bar{p}}(t) \phi_p(t)$$

Then equation III.12 can be rewritten in terms of the meson-meson operators.

$$C_{\bar{p}\bar{q}}^{(4)}(t, t_0) = \langle \Phi_{\bar{p}}^+(t) \Phi_{\bar{q}}(t_0) \rangle_U - \langle \Phi_{\bar{p}}^+(t) \rangle_U \langle \Phi_{\bar{q}}(t_0) \rangle_U \quad (\text{III.13})$$

There are two results which greatly simplify our work in calculating this correlation function. Because of the fermion flavour (u,d) assignments, all separable terms in this expression vanish. Furthermore, all contractions within each of the meson-meson operators, $\Phi_{\bar{p}}^+(t)$ or $\Phi_{\bar{q}}(t_0)$ operator are identically zero. Therefore, we are left with only four possible sets of contractions in the calculation.

$$\begin{aligned}
G_4(x_1x_2y_1y_2) = & \langle :\bar{\chi}(x_2)\chi(x_1): :\chi(x_2)\bar{\chi}(x_1): :\bar{\chi}(y_2)\chi(y_1): :\chi(y_2)\bar{\chi}(y_1): \rangle \\
& + \langle :\bar{\chi}(x_2)\chi(y_1): :\chi(x_2)\bar{\chi}(y_1): :\bar{\chi}(y_2)\chi(x_1): :\chi(y_2)\bar{\chi}(x_1): \rangle \\
& - \langle :\bar{\chi}(x_2)\chi(x_1): :\chi(x_2)\bar{\chi}(y_1): :\bar{\chi}(y_2)\chi(y_1): :\chi(y_2)\bar{\chi}(x_1): \rangle \\
& - \langle :\bar{\chi}(x_2)\chi(y_1): :\chi(x_2)\bar{\chi}(x_1): :\bar{\chi}(y_2)\chi(x_1): :\chi(y_2)\bar{\chi}(y_1): \rangle \quad (\text{III.14})
\end{aligned}$$

In terms of the inverse fermion matrix G_{xy} , we have

$$\begin{aligned}
G_4(x_1x_2y_1y_2) = & \langle (G_{x_2x_1})(G_{x_2x_1})^*(G_{y_2y_1})(G_{y_2y_1})^* \rangle_U \\
& + \langle (G_{x_2y_1})(G_{x_2y_1})^*(G_{y_2x_1})(G_{y_2x_1})^* \rangle_U \\
& - \langle (G_{x_2x_1})(G_{x_2y_1})^*(G_{y_2y_1})(G_{y_2x_1})^* \rangle_U \\
& - \langle (G_{x_2y_1})(G_{x_2x_1})^*(G_{x_2y_1})(G_{y_2y_1})^* \rangle_U \quad (\text{III.15})
\end{aligned}$$

where x , x , y and y represent 2+1 dimensional lattice spacetime points on the left-hand-side of equation III.15 and the corresponding elements of the inverse fermion matrix G on the right-hand-side of the equation.

As before, we Fourier transform and then express our result in center-of-mass momenta, \mathbf{P} and \mathbf{Q} , and relative momenta, \mathbf{p} and \mathbf{q} .

$$L^{-8} \sum_{\vec{x}_1} \sum_{\vec{x}_2} \sum_{\vec{y}_1} \sum_{\vec{y}_2} e^{i(\frac{1}{2}\vec{P}+\vec{p})\vec{x}_1} e^{i(\frac{1}{2}\vec{Q}+\vec{q})\vec{y}_1} e^{i(\frac{1}{2}\vec{P}-\vec{p})\vec{x}_2} e^{i(\frac{1}{2}\vec{Q}-\vec{q})\vec{y}_2} G_4(x_1, x_2, y_1, y_2) \quad (\text{III.16})$$

Again going to the center-of-momentum frame,

$$C_{\vec{p}\vec{q}}^4(t, t_0) = L^{-8} \sum_{\vec{x}_1} \sum_{\vec{x}_2} \sum_{\vec{y}_1} \sum_{\vec{y}_2} e^{i\vec{p}(\vec{x}_1 - \vec{x}_2)} e^{i\vec{q}(\vec{y}_1 - \vec{y}_2)} G_4(x_1, x_2, y_1, y_2) \quad (\text{III.17})$$

Now, we substitute our previous result III.15 into equation III.17 and obtain

$$\begin{aligned} C_{\vec{p}\vec{q}}^4(t, t_0) &= L^{-8} \sum_{\vec{x}_1} \sum_{\vec{x}_2} \sum_{\vec{y}_1} \sum_{\vec{y}_2} e^{i\vec{p}(\vec{x}_1 - \vec{x}_2)} e^{i\vec{q}(\vec{y}_1 - \vec{y}_2)} \\ &< (G_{\vec{x}_2 t, \vec{x}_1 t_0})(G_{\vec{x}_2 t, \vec{x}_1 t_0})^* (G_{\vec{y}_2 t, \vec{y}_1 t_0})(G_{\vec{y}_2 t, \vec{y}_1 t_0})^* \\ &+ (G_{\vec{x}_2 t, \vec{y}_1 t_0})(G_{\vec{x}_2 t, \vec{y}_1 t_0})^* (G_{\vec{y}_2 t, \vec{x}_1 t_0})(G_{\vec{y}_2 t, \vec{x}_1 t_0})^* \\ &- (G_{\vec{x}_2 t, \vec{x}_1 t_0})(G_{\vec{x}_2 t, \vec{y}_1 t_0})^* (G_{\vec{y}_2 t, \vec{y}_1 t_0})(G_{\vec{y}_2 t, \vec{x}_1 t_0})^* \\ &- (G_{\vec{x}_2 t, \vec{y}_1 t_0})(G_{\vec{x}_2 t, \vec{x}_1 t_0})^* (G_{\vec{y}_2 t, \vec{x}_1 t_0})(G_{\vec{y}_2 t, \vec{y}_1 t_0})^* >_U \quad (\text{III.18}) \end{aligned}$$

A quite intuitive physical interpretation of this equation can easily be obtained from looking at figure III.1.

To simplify later discussions, equation III.18 will be rewritten in the form

$$C^{(4)} = C^{(4A)} + C^{(4B)} - C^{(4C)} - C^{(4D)} \quad (\text{III.19})$$

The terms $C^{(4A)}$ and $C^{(4B)}$ are separable and thus relatively easy to compute, although we do

require the entire inverse fermion matrix G rather than just one column for this calculation.

3. Properties of the 4-Point Time Correlation Function

The four-point time correlation matrix possesses several symmetries of which we can later take advantage in order to greatly simplify our numerical work.

- (1) The matrix is Hermitean

$$C_{\vec{p}\vec{q}}^4 = C_{\vec{q}\vec{p}}^{4*} \quad (\text{III.20})$$

- (2) Renaming the dummy summation indices simultaneously

$$\vec{x}_1 \leftrightarrow \vec{x}_2 \quad \text{and} \quad \vec{y}_1 \leftrightarrow \vec{y}_2$$

reveals several symmetries of the individual terms

$$C_{\vec{p}\vec{q}}^{(4A)} = C_{\vec{p}\vec{q}}^{(4A)*}$$

$$C_{\vec{p}\vec{q}}^{(4B)} = C_{\vec{p}\vec{q}}^{(4B)*}$$

$$C_{\vec{p}\vec{q}}^{(4C)} = C_{\vec{p}\vec{q}}^{(4D)*} \quad (\text{III.21})$$

These symmetries allow us to rewrite the four-point time-correlation function in the form

$$C_{\vec{p}\vec{q}}^4 = C_{\vec{p}\vec{q}}^{(4A)} + C_{\vec{p}\vec{q}}^{(4B)} - 2\Re C_{\vec{p}\vec{q}}^{(4C)} \quad (\text{III.22})$$

which makes the calculation of the matrix elements easier.

(3) Renaming the dummy summation indices simultaneously reveals

$$C_{\vec{p},\vec{q}}^4 = C_{-\vec{p},\vec{q}}^4 = C_{\vec{p},-\vec{q}}^4 = C_{-\vec{p},-\vec{q}}^4 \quad (\text{III.23})$$

These last symmetries reduce the range of momenta for which matrix elements of $C^{(4)}$ need to be calculated from $L^2 = (24)^2 = 576$ to only $\frac{1}{2}L(L+1) + 1 = 301$.

4. The Truncated Time-Correlation Matrix

Furthermore, it is expected that low-lying energy levels will be determined mainly by matrix elements with small momentum indices. So, due to limitations of computer resources, we will take advantage of this fact to calculate only a truncated matrix C for the set of momenta

$$\vec{p} = \frac{2\pi}{L}(k_1, k_2) \quad \text{where} \quad |k_{1,2}| \leq 2 \quad (\text{III.24})$$

rather than calculating the full 301×301 matrix $C^{(4)}$. The selected values of the momentum are indicated in figure III.2.

5. Notes

This discussion follows Fiebig, Woloshyn and Domínguez (1994). Fetter & Walecka (1971) explains the concept of contraction, as well as Wick's Theorem.

1,2. Fiebig, Woloshyn and Domínguez (1994).

$$C^{(4A)} + C^{(4B)} - C^{(4C)} - C^{(4D)} =$$

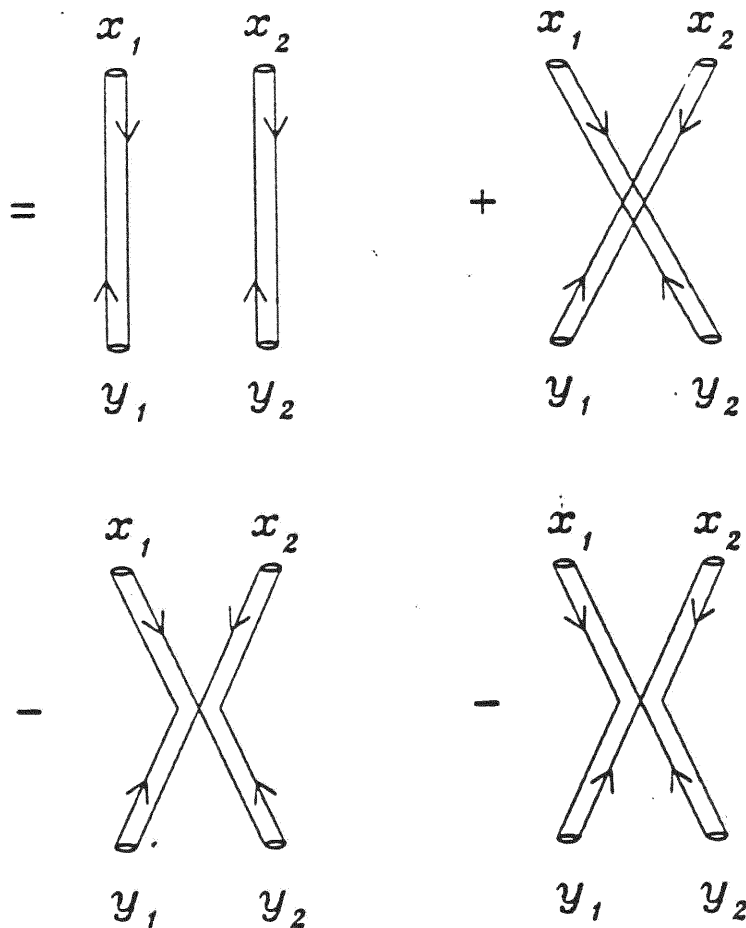


FIGURE III.1
ILLUSTRATION OF EQUATION 3.18

Diagrammatic representation of the four types of contractions that contribute to the four-point correlation functions $C^{(4)}$, as explained in the text in equations III.17 and III.18.

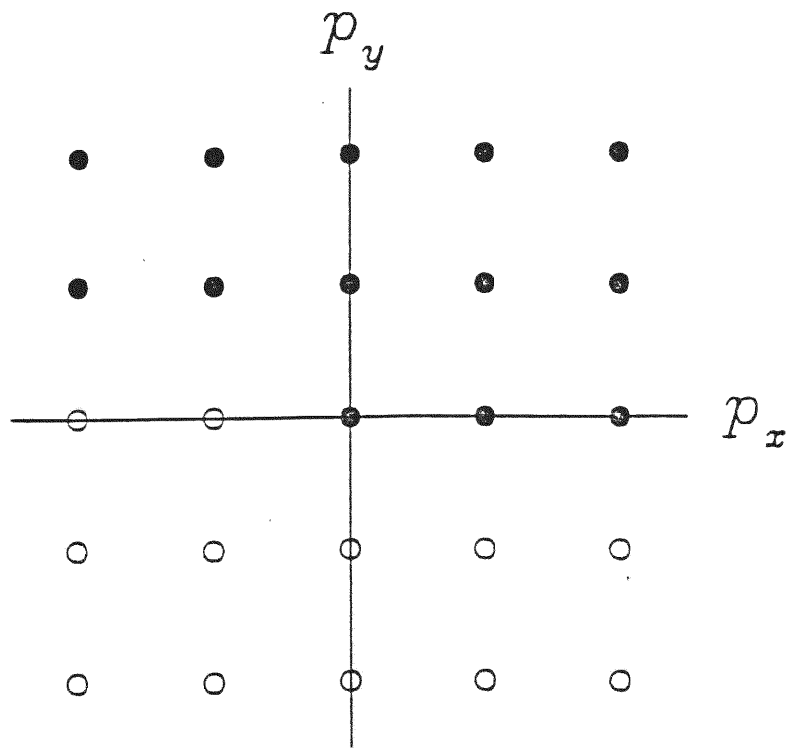


FIGURE III.2
RANGE OF MOMENTA

The filled circles indicate the values of the momentum for which we need to calculate $C^{(4)}$ once the symmetries in equations (III.20) through (III.23) are taken into account. This is indicated in equation (III.24) and discussed in the text in sections III.3, III.4 and IV.3.

IV. NUMERICAL RESULTS

1. Random-Source Technique

We are now faced with a prohibitive sum over $L^2 \approx 10^{11}$ terms to obtain the correlation matrix. It becomes necessary to introduce a random-source technique, so that we can use a Monte Carlo statistical estimator which requires far less in the way of computing resources. The random-source technique begins with defining random complex Gaussian vectors R (called the random-source vectors) of length L^2 on space sites $\mathbf{x} \in Z^2$ subject to the orthonormality condition¹

$$\sum_{\langle R \rangle} R_{\mathbf{x}}^* R_{\mathbf{y}} = \delta_{\mathbf{x}\mathbf{y}} \quad (\text{IV.1})$$

where $\langle R \rangle$ denotes a statistical average over an ensemble of random vectors.

Next we define vectors H (called the Fourier-modified random-source vectors) by

$$H_{\mathbf{x}t, t_0}(\vec{p}, R) = L^{-2} \sum_{\mathbf{y}} G_{\mathbf{x}t, \mathbf{y}t_0} e^{i\vec{p}\mathbf{y}} R_{\mathbf{y}} \quad (\text{IV.2})$$

These vectors H have the property that

$$\sum_{\langle R \rangle} H_{\mathbf{x}t, t_0}(\vec{q}, R)^* H_{\mathbf{y}t, t_0}(\vec{p}, R) = L^{-4} \sum_{\mathbf{z}} G_{\mathbf{x}\mathbf{z}, t_0}^* e^{i(\vec{p}-\vec{q})\mathbf{z}} G_{\mathbf{y}\mathbf{z}, t_0} \quad (\text{IV.3})$$

2. Time Correlation Functions

Using the random-source technique described above, we can obtain an expression for the two-point time-correlation function.²

$$C^{(2)}(t, t_0) = \left\langle \sum_{\langle R \rangle} \sum_{\vec{x}} |H_{\vec{x}, t_0}(\vec{p}, R)|^2 \right\rangle_U \quad (\text{IV.4})$$

To obtain an expression for the four-point time-correlation function requires generating two independent random vectors R^1 and R^2 due to the presence of four G factors.

The various contributions to the four-point time-correlation functions are³

$$C_{\vec{p}\vec{q}}^{(4A)}(t, t_0) = \left\langle \sum_{\langle R^1 \rangle} \sum_{\vec{x}_1} e^{i\vec{p}\cdot\vec{x}_1} H_{\vec{x}_1, t_0}(\vec{q}, R^1) H_{\vec{x}_1, t_0}^*(\vec{0}, R^1) \right. \\ \left. \sum_{\langle R^2 \rangle} \sum_{\vec{x}_2} e^{i\vec{p}\cdot\vec{x}_2} H_{\vec{x}_2, t_0}(\vec{0}, R^2) H_{\vec{x}_2, t_0}^*(\vec{q}, R^2) \right\rangle_U$$

$$C_{\vec{p}\vec{q}}^{(4B)}(t, t_0) = \left\langle \sum_{\langle R^1 \rangle} \sum_{\vec{x}_2} e^{i\vec{p}\cdot\vec{x}_2} H_{\vec{x}_2, t_0}(\vec{0}, R^1) H_{\vec{x}_2, t_0}^*(\vec{q}, R^1) \right. \\ \left. \sum_{\langle R^2 \rangle} \sum_{\vec{x}_1} e^{i\vec{p}\cdot\vec{x}_1} H_{\vec{x}_1, t_0}(\vec{q}, R^2) H_{\vec{x}_1, t_0}^*(\vec{0}, R^2) \right\rangle_U$$

$$C_{\vec{p}\vec{q}}^{(4C)}(t, t_0) = \left\langle \sum_{\langle R^1 \rangle} \sum_{\langle R^2 \rangle} \sum_{\vec{x}_1} H_{\vec{x}_1, t_0}(\vec{0}, R^1) H_{\vec{x}_1, t_0}^*(\vec{0}, R^2) \right. \\ \left. \sum_{\vec{x}_2} e^{i\vec{p}\cdot\vec{x}_2} H_{\vec{x}_2, t_0}(\vec{q}, R^2) H_{\vec{x}_2, t_0}^*(\vec{q}, R^1) \right\rangle_U$$

3. Our Choice of Parameters

The gauge field configurations were generated using the molecular dynamics algorithm⁴. Although this algorithm is capable of dealing with dynamical fermions, we used the so-called quenched approximation, in which closed fermion loops are ignored.

$$Z = \int [dU] (\det G[U])^{N_F} e^{-S_F[U]} \rightarrow \int [dU] e^{-S_F[U]}$$

The bare fermion mass was taken to be $m_F = 0.1$.

Quantum chromodynamics is a confined theory; i. e., the particles of the theory, quarks and gluons, do not appear free in nature. Whether a lattice theory is confined or deconfined depends on the value used for the coupling constant g , or $\beta = 1/2g^2$. We need to perform our calculations using a value of β for which the quarks are confined. Otherwise, we would have a sort of free quark gas rather than the two asymptotic bound meson-like particles with which we want to work. Figure IV.2 provides a schematic description of confinement and deconfinement in QED and QCD. QCD is confined for all values of the coupling parameter β . Lattice QED₂₊₁, on the other hand, displays a confinement-deconfinement phase transition, indicated by the value of the coupling parameter $\beta = \beta_c$. We must use a value of β for QED₂₊₁ for which that theory is confined, so that it simulates the behavior of QCD.

Confinement in a lattice theory is indicated numerically by the value of the Wilson line $\langle W \rangle \sim e^{-|V(x)|}$. The value of the Wilson line is small when the value for the potential is large, which occurs in a bound (confined) state, and large when the value for the potential is small, indicating a free particle state. In turn, the value of the potential depends on the choice for coupling parameter β . On an $8^2 \times 12$ lattice, the value $\beta = 1.5$ gives a value for the Wilson line of about 0.1 (see figure IV.1), which marks the onset of the deconfinement phase transition for QED₂₊₁. However, by using a $24^2 \times 32$ lattice, the same value $\beta = 1.5$ yields a much lower value of about 0.03 for the Wilson line, which is now far into the confined

region. An additional benefit of using the QED_{2+1} model in order to accommodate a larger lattice is thus realized.

The coupling parameter was taken to be $\beta=1.5$.

Since the energy levels are extracted from the exponential decay of the correlation matrix with time, the lattice must be fairly large along the time axis. The length of the time axis was taken to be $L_t = 32$.

As mentioned in the introduction, our lattice had to be large enough in the space dimensions to accommodate two slowly-moving composite meson-like particles. Calculations of the single-meson mass seem to indicate that a single meson is accommodated with sufficient accuracy in a lattice with $L \approx 12$ (see figure IV.3). Therefore, a lattice twice this size should be sufficient for our purposes.

The linear dimensions of the lattice were taken to be $L^2=24 \times 24$.

We needed to solve the equation for the 13 values of the momentum (see Figure III.2), while the random vector R was kept fixed. A new set of 16 random vectors was generated for each of the 64 different gauge field configurations which we had generated. This means we needed to call our solver subroutine a total of 13312 times. And, on our $24^2 \times 32$ lattice, this subroutine is being used to solve a 18432 by 18432 matrix.

4. The Lattice Simulation Procedure

We now wish to obtain the time propagation of the Fourier-modified random source $H_{\vec{x},t_0}(\vec{p},R)$. We do this by applying a conjugate gradient solver routine⁵ to the equation

$$\sum_{\vec{x}_0} G_{\vec{y}_0, \vec{x}_0}^{-1} X_{\vec{x}_0} = L^{-2} e^{i\vec{p}\cdot\vec{y}} R_{\vec{y}} \delta_{\vec{y}_0 t_0}$$

The solution X to this equation is related to the H-vector by

$$H_{\vec{x}, t_0}(\vec{p}, R) = X_{\vec{x}t}$$

For the four-point time-correlation function, the minimal procedure which can be followed is to use vectors 1 to 8 as $R^{(1)}$ and vectors 9 to 16 as $R^{(2)}$ for one calculation of $C^{(4)}(t, t_0)$ and then assign vectors 9 to 16 as $R^{(1)}$ and vectors 1 to 8 as $R^{(2)}$ and make a second calculation. However, there is a more sophisticated procedure which improves the suppression factor for the error of the R-estimator. We can subdivide the 16 vectors into groups of four vectors. There are six independent ways of assigning 2 of these 4 groups to $R^{(1)}$ and the remaining 2 groups to $R^{(2)}$. The averages obtained from these six assignments are then used to calculate the four-point time-correlation function.

5. The Numerical Results

The lattice on which we have set up our theory obeys the point symmetries of the square symmetry group $O(2, Z)$. The group $O(2, Z)$ has five irreducible representations. In chapter VI and appendix B, we will discuss the group and its representations in detail. But for the purposes of explaining the numerical results, it will suffice to say that these representations are denoted by A_1 , A_2 , B_1 , B_2 and E. The first four of these are one-dimensional representations, and the last is a two-dimensional representation.

Figures IV.4 and figure IV.5 show the various contributions to the truncated reduced

four-point correlation matrix indicated by equation III.22. Figure IV.4 shows the $C^{(4A)}$, $C^{(4B)}$ and $C^{(4C)}$ contributions in the A_1 sector. It also shows the $C^{(4B)}$ contributions in the A_2 sector, where the $C^{(4A)}$ and $C^{(4C)}$ contributions are zero. Figure IV.5 shows the $C^{(4B)}$ contribution in the B_1 and B_2 sectors, where the $C^{(4A)}$ and $C^{(4C)}$ contributions are also zero. All the reduced matrix elements in the two-dimensional E-sector are identically zero because of the symmetries of the reduced matrix discussed in section III.3. This is discussed at greater length in Chapter VI and appendix B.

The large-time behavior of the square of the two-point time-correlation function is (see figure IV.6)

$$C_{\vec{p}=0}^{(2)}(t,t_0)^2 \approx c_0 \cosh 2m(t-t_c) \quad \text{where } t=t_c=17 \quad (\text{IV.5})$$

The results obtained from the two-parameter (c_0 and $2m$) least-squares fit to equation IV.5 are shown in table I. We now turn to the problem of finding the energy levels W_n of the interacting two-body system.

We do this by solving the eigenvalue equation in each of the four sectors A_1 , A_2 , B_1 and B_2 . (Again, we will not need to solve the equation in the E sector because all the reduced matrix elements in the E-sector are identically zero.)

$$\sum_{q^2} C_{p^2q^2}(t,t_0) v_{q^2}^{(n)}(t,t_0) = \lambda_n(t,t_0) v_{q^2}^{(n)}(t,t_0)$$

The eigenvalues $\lambda_n(t,t_0)$ behave like

$$\lambda_n(t,t_0) \approx c_n \cosh[W_n(t-t_c)] \quad \text{where } t=t_c=17 \quad (\text{IV.6})$$

The leading correction term to this equation is of order $O(\Delta W_n(t, t_0) \sinh[W_n(t-t_0)])$ where ΔW_n is the distance to the next closest energy level. The eigenvalue functions $\lambda_n(t, t_0)$ are shown in figures IV.7 through IV.10. The results of the two-parameter (c_n and W_n) least-squares fit to all the eigenvalues IV.6 in each of the four sectors are also shown in table I.

Finally, from the results for W_n , we obtain the squares of the relative momenta from the equation

$$k_n^2 = (W_n^2 - (2m)^2)/2 \quad (\text{IV.7})$$

This gives us a total of eleven momenta usable in the phase shift calculation. The values of k_n^2 obtained from using our values of W_n in equation IV.7 are shown in table I.

6. Notes

A much more detailed explanation of the numerical work, including an error analysis, can be found in Fiebig, Woloshyn and Domínguez (1994). The molecular dynamics algorithm is explained in Gottlieb et al (1987). Most of the relevant numerical analysis background can be found in Beckman (1960), which includes an explanation of the conjugate-gradient solver, and Efron (1979), which includes a discussion of the error analysis. An explanation of the Wilson line can already be found in Wilson (1974).

1. Gottlieb et al (1987).
Scallear, Scalopino and Sugar (1986).
2. Fiebig, Woloshyn and Domínguez (1994).
3. Fiebig, Woloshyn and Domínguez (1994).

4. Gottlieb et al (1987).
Fiebig, Woloshyn and Domínguez (1994).
5. Beckman (1960).
Fiebig, Woloshyn and Domínguez (1994).

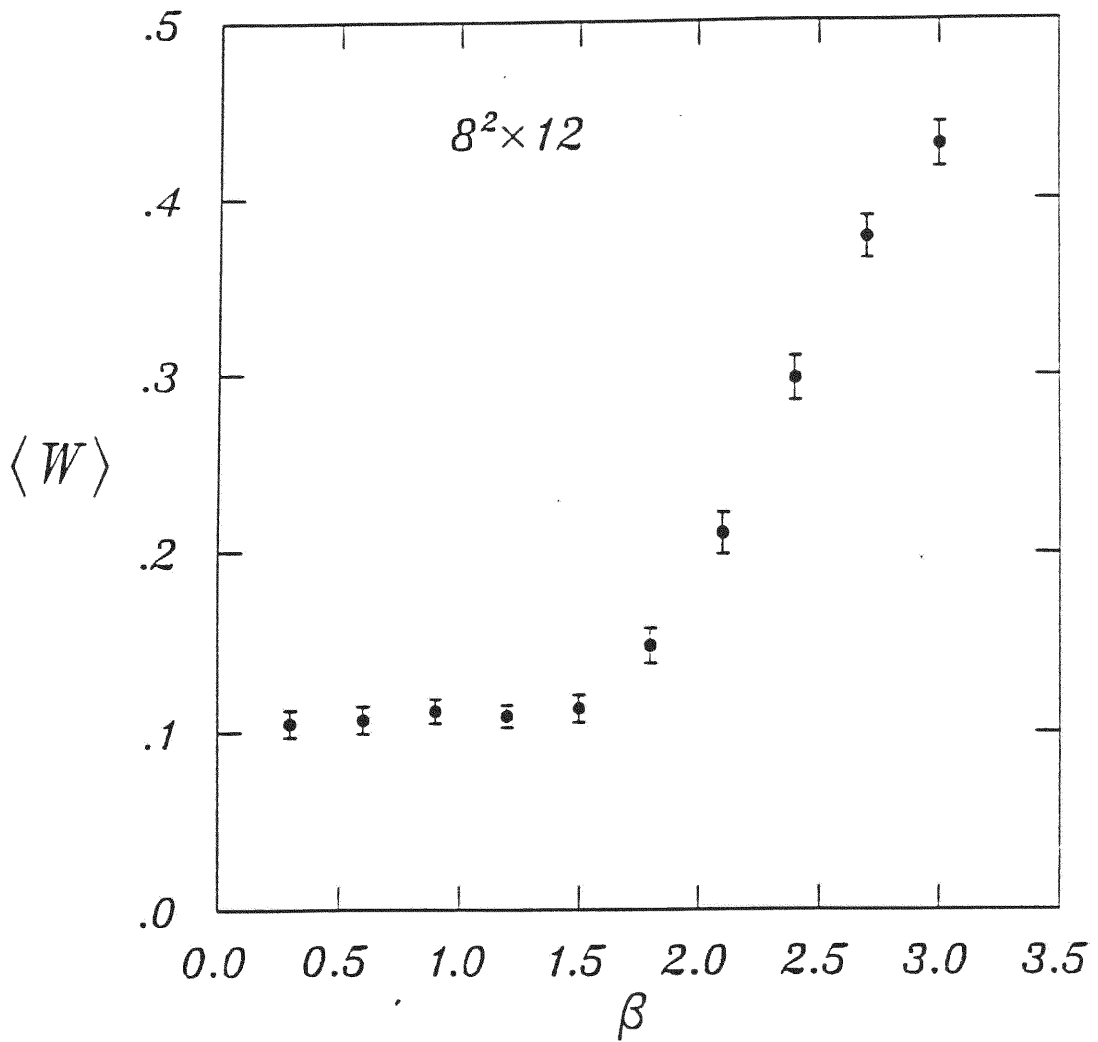


FIGURE IV.1
WILSON LINE VERSUS COUPLING PARAMETER

The Wilson line $\langle W \rangle$ versus the coupling parameter β for an $8^2 \times 12$ lattice, using the value $m_f = 0.1$. The data were obtained from 64 gauge configurations, 128 trajectories apart.

Quantum Chromodynamics in 3 + 1 Dimensions:



Quantum Electrodynamics in 2 + 1 Dimensions (on a $8^2 \times 12$ Lattice)



Quantum Electrodynamics in 2 + 1 Dimensions (on a $24^2 \times 32$ Lattice)



FIGURE IV.2
CONFINEMENT AND DECONFINEMENT IN QCD AND QED

A schematic illustration of confinement and deconfinement in lattice QED on lattices of two different sizes. The bold lines represent values of the coupling parameter for which QED is confined. The significance of this is discussed in the text in section IV.3.

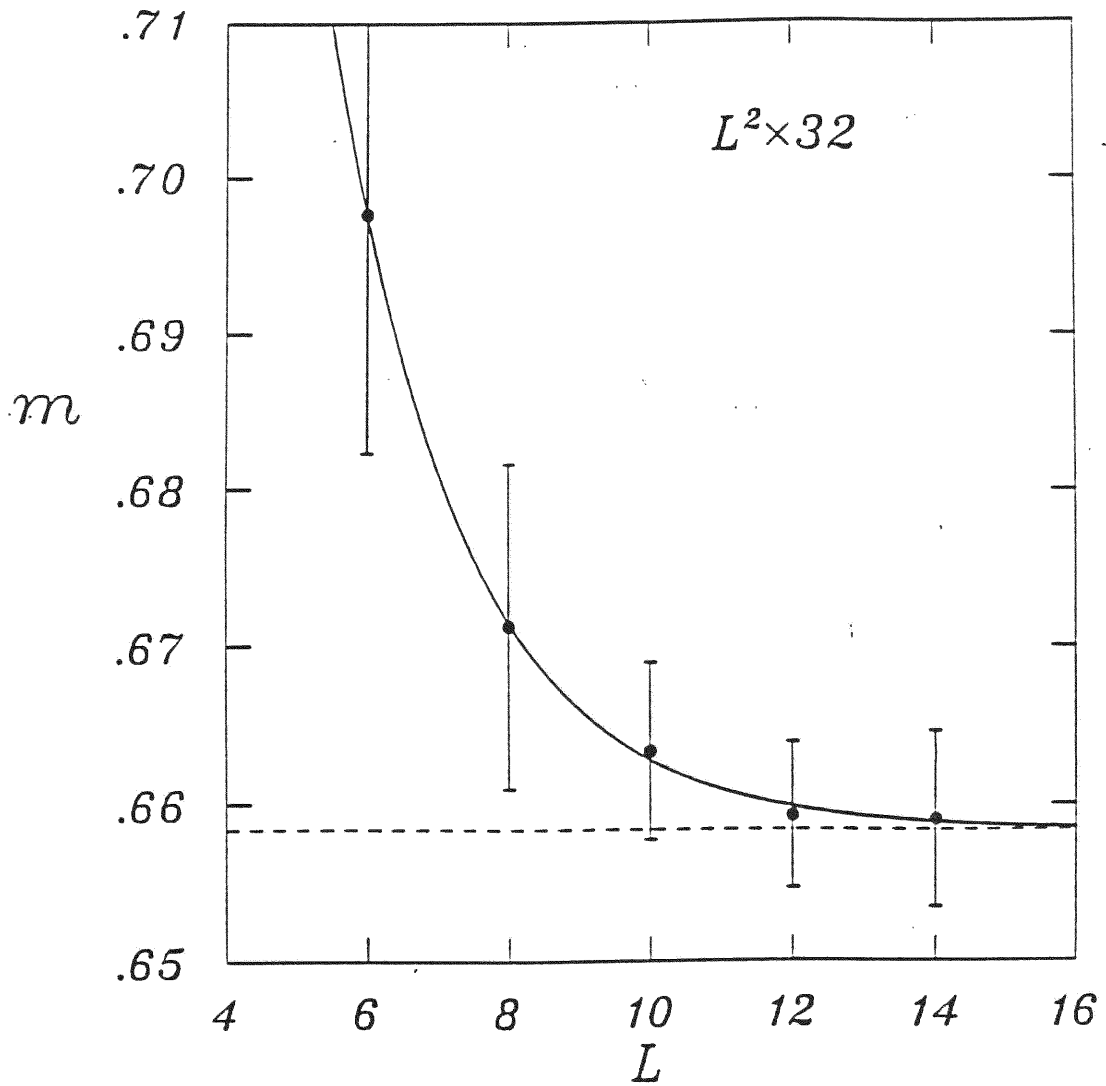


FIGURE IV.3
MESONIC MASS VERSUS L

The mass m of a single meson versus L for $L^2 \times 32$ lattices, using the values $m_f = 0.1$ for the bare fermion mass and $\beta = 1.5$ for the coupling parameter. The data were obtained from 64 gauge configurations, 128 trajectories apart.

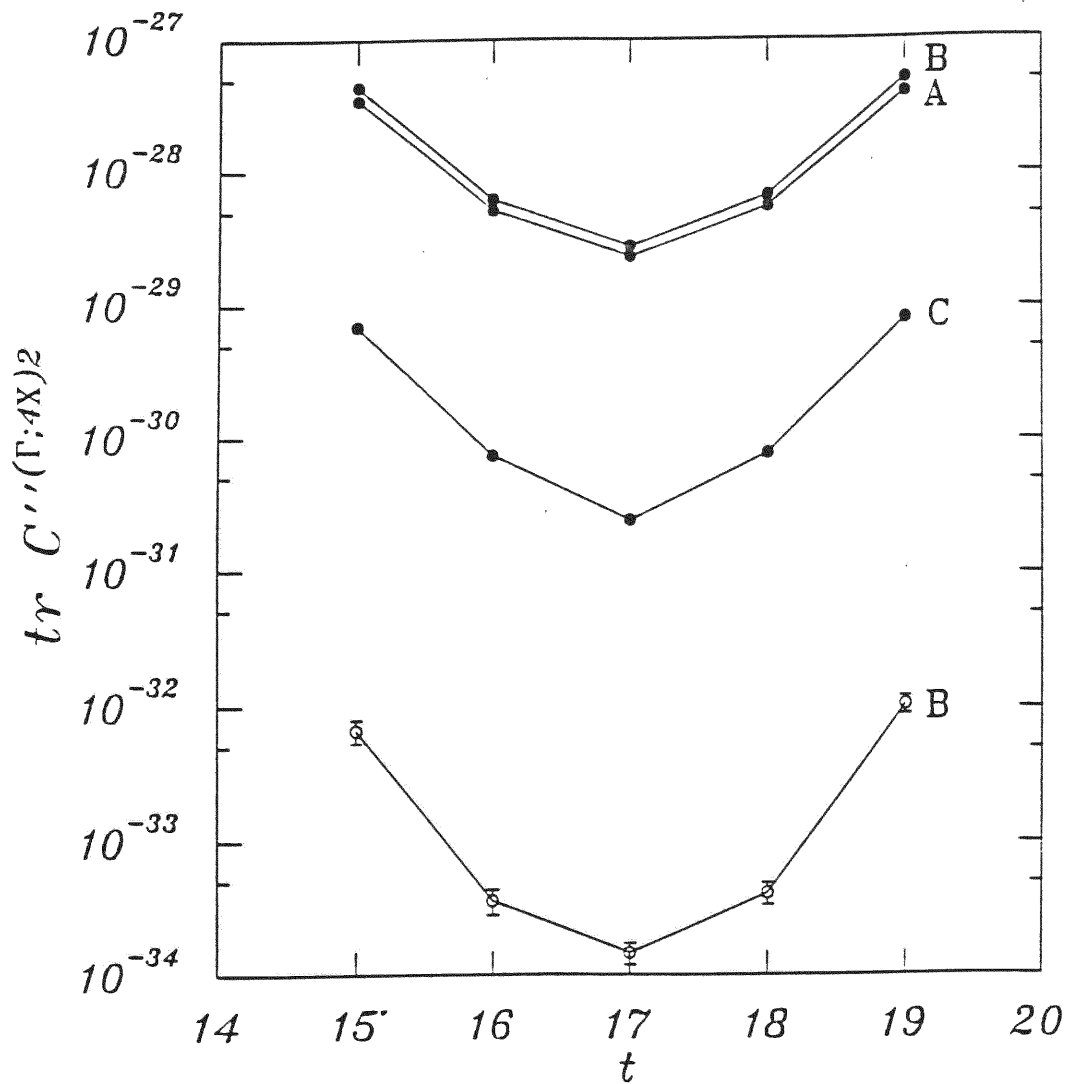


FIGURE IV.4
CONTRIBUTIONS TO C'' IN A_1 AND A_2

The graph shows the traces of the squares of the various contributions $C''(\Gamma; 4X)$ to the truncated reduced four-point correlation matrix, as discussed in sections III.3 and IV.5 of the text. The representations for the A_1 sector are given by filled plot symbols, and the representations for the A_2 sector are given by open plot symbols.

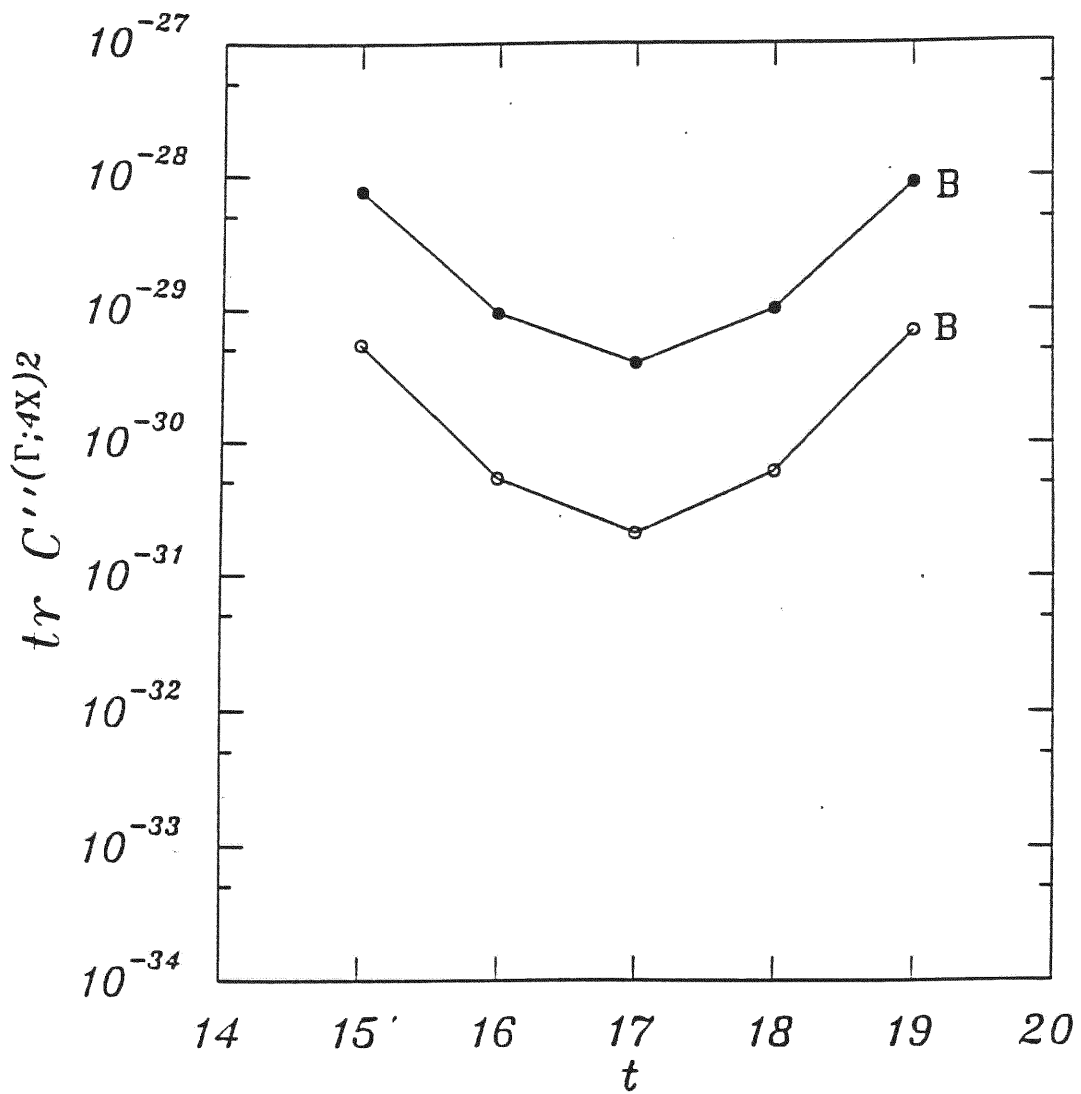


FIGURE IV.5
CONTRIBUTIONS TO C^r IN B_1 AND B_2

The graph shows the traces of the squares of the various contributions $C^{(\Gamma;4X)}$ to the truncated reduced four-point correlation matrix, as discussed in sections III.3 and IV.5 of the text. The representations for the B_1 sector are given by filled plot symbols, and the representations for the B_2 sector are given by open plot symbols.

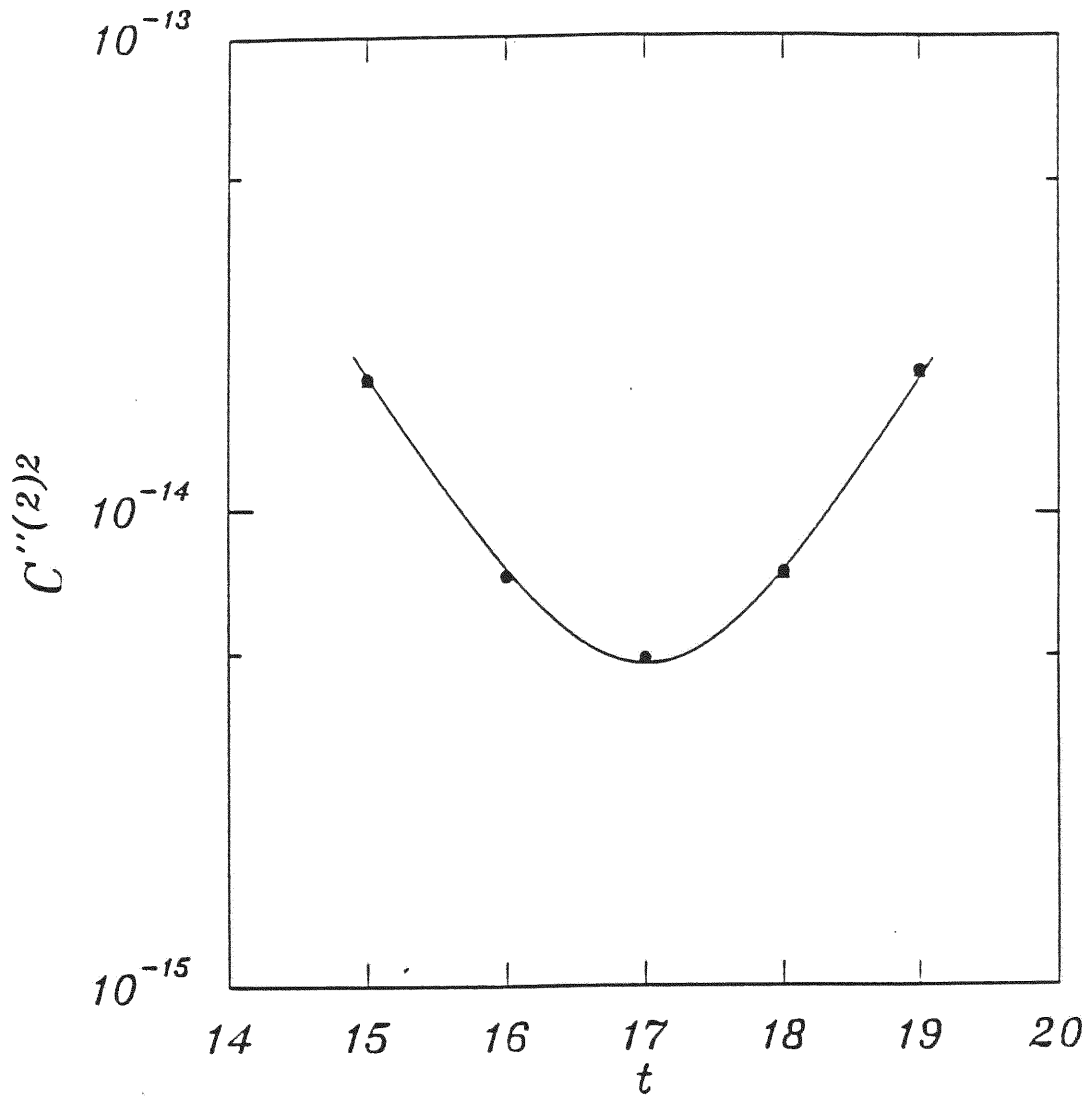


FIGURE IV.6
ILLUSTRATION OF EQUATION IV.5

A two-parameter least-squares fit to the square of the two-point correlation function according to equation IV.5. The numerical results for c_0 and m given by this fit are shown in table I.

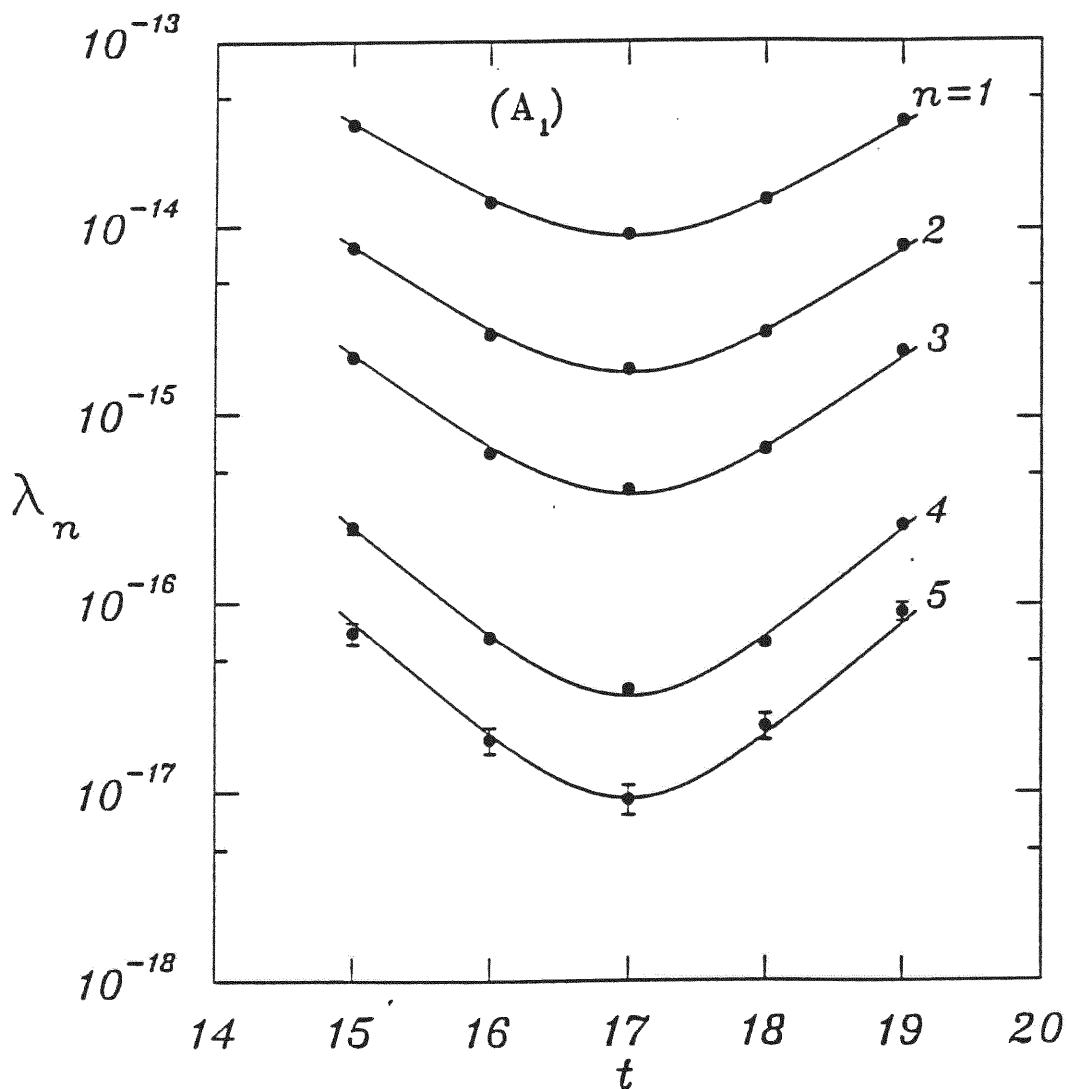


FIGURE IV.7
EIGENVALUES IN A₁

The graph shows the time dependence of the eigenvalues $\lambda_n(t, t_0)$ of the four-point correlation matrix in the A₁ sector for the first five energy levels. The curves are two-parameter least-squares fits according to equation IV.6. The data for $n=6$ could not be fit to a curve because of the large error bars and have therefore not been included.

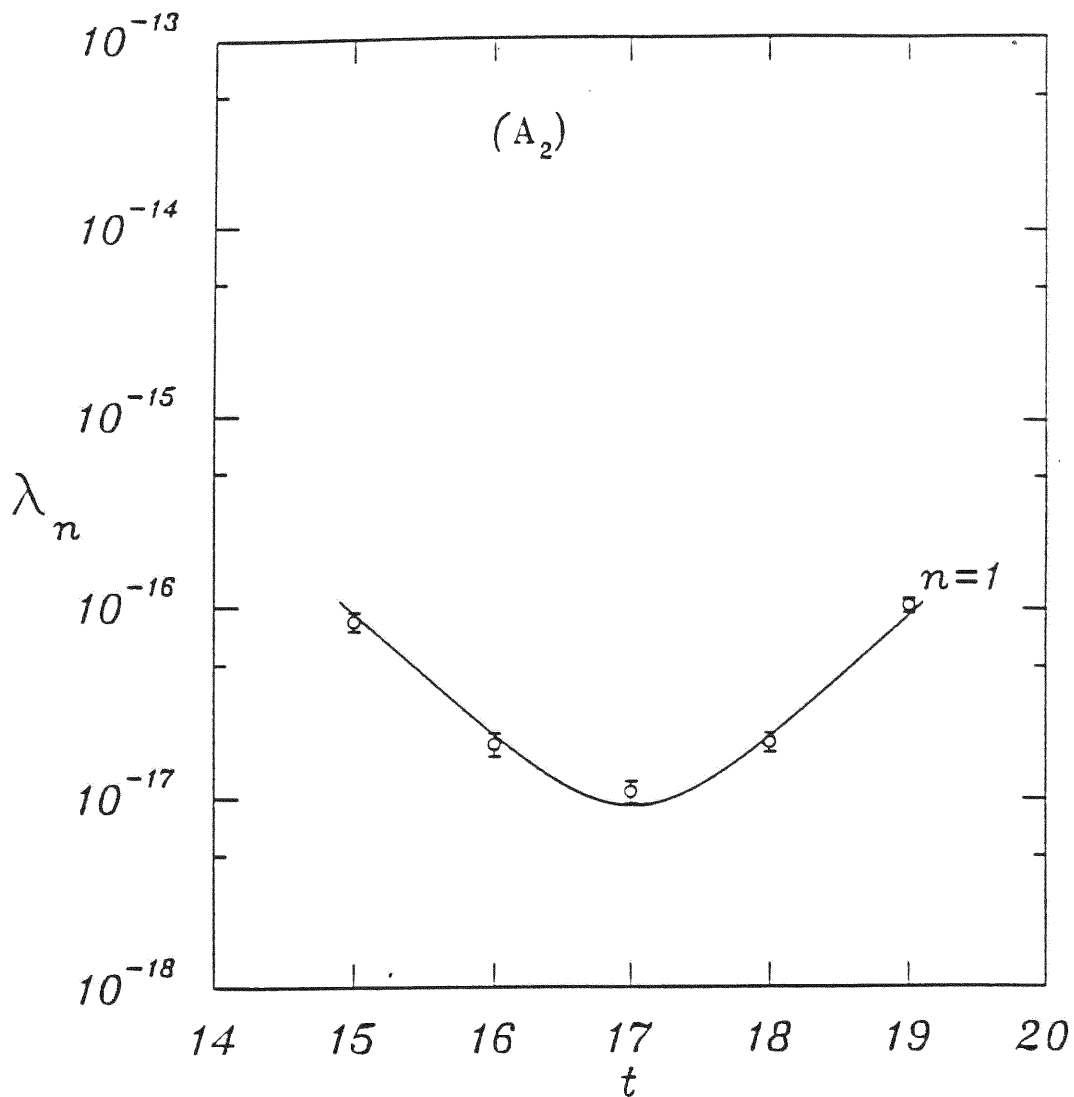


FIGURE IV.8
EIGENVALUES IN A_2

The graph shows the time dependence of the eigenvalue $\lambda_n(t, t_0)$ of the four-point correlation matrix in the A_2 sector for the first energy level. The curve is a two-parameter least-squares fit according to equation IV.6.

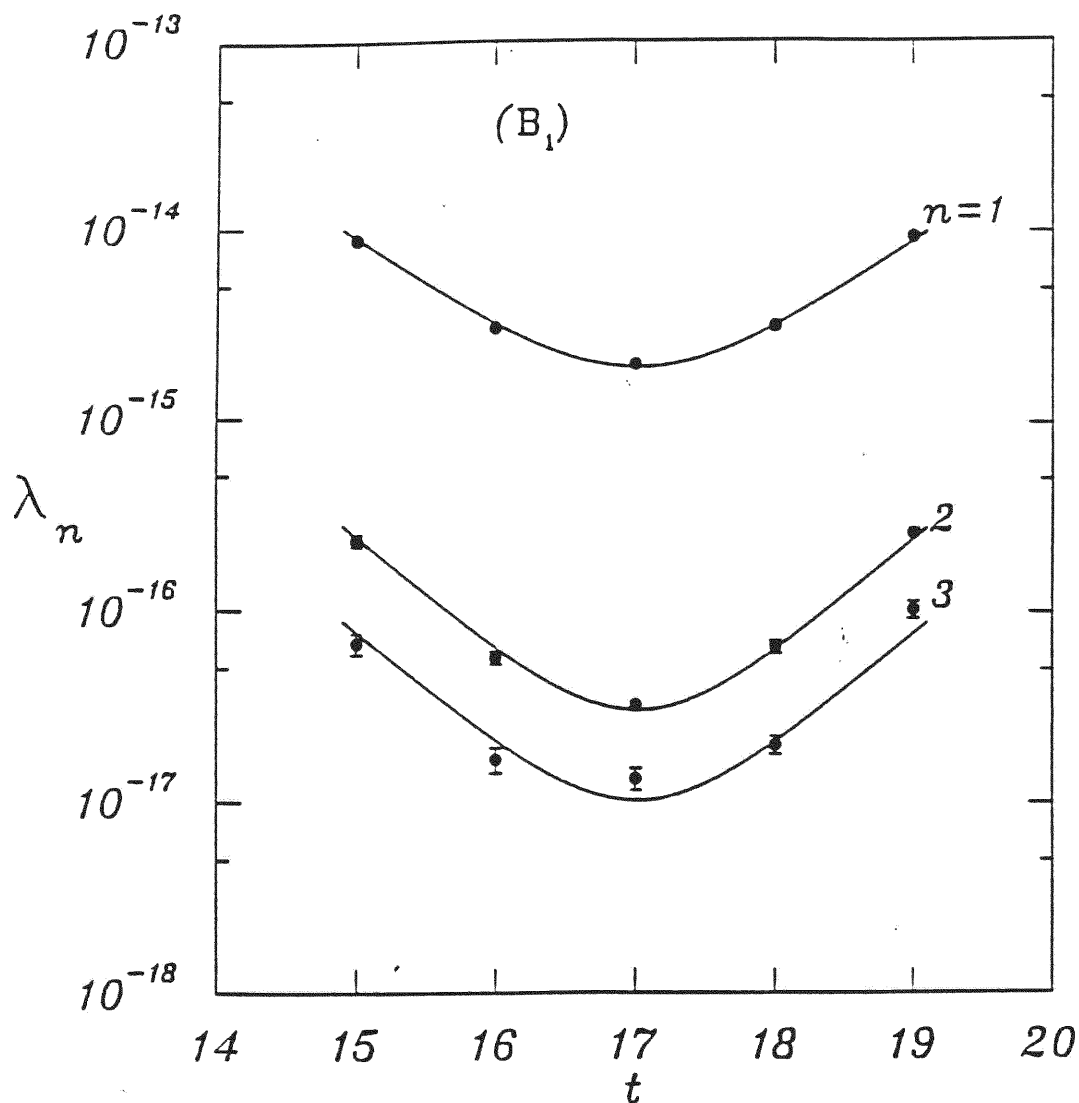


FIGURE IV.9
EIGENVALUES IN B₁

The graph shows the time dependence of the eigenvalues $\lambda_n(t, t_0)$ of the four-point correlation matrix in the B₁ sector for the first three energy levels. The curves are two-parameter least-squares fits according to equation IV.6.

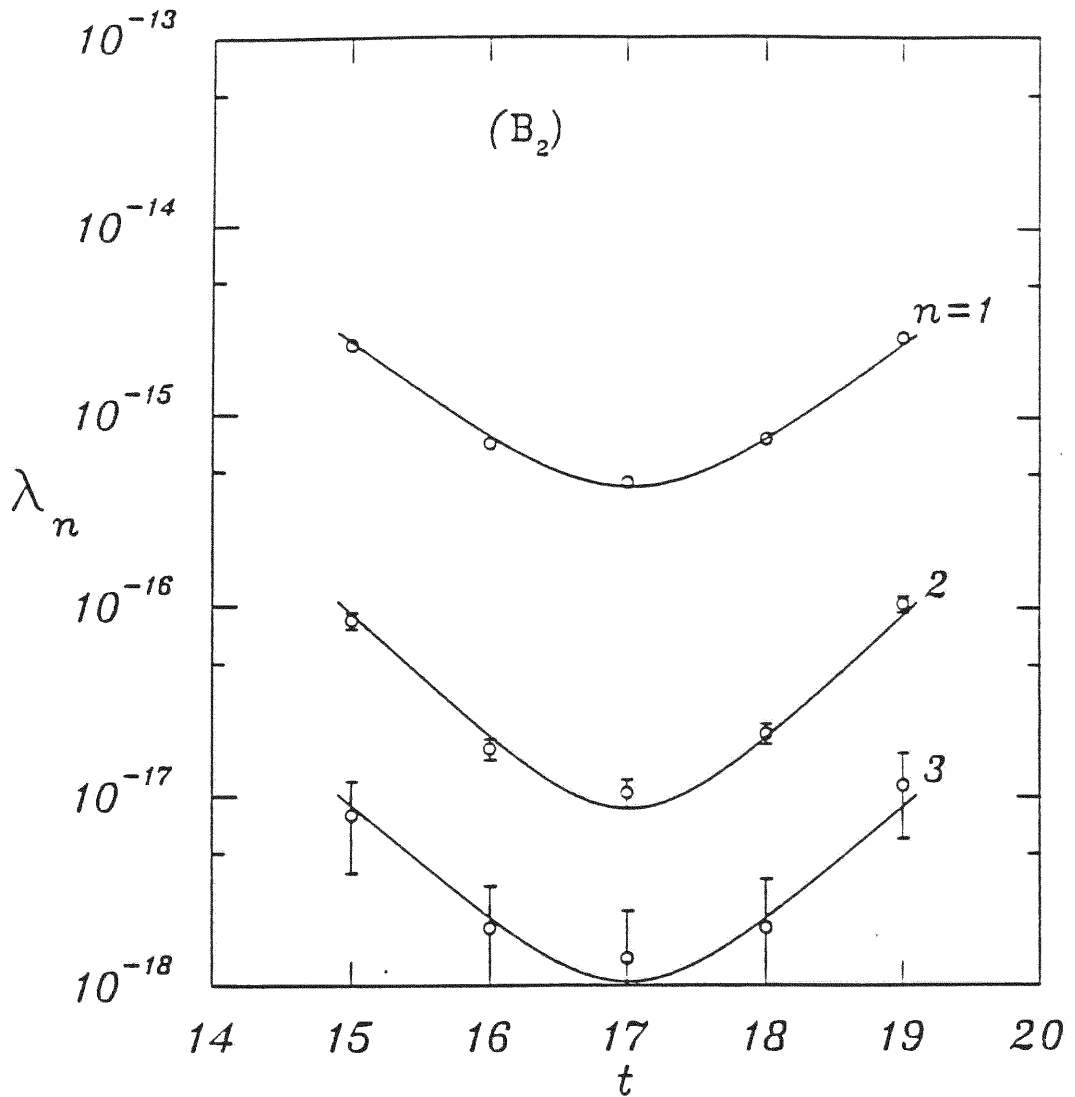


FIGURE IV.10
EIGENVALUES IN B₂

The graph shows the time dependence of the eigenvalues $\lambda_n(t, t_0)$ of the four-point correlation matrix in the B₂ sector for the first three energy levels. The curves are two-parameter least-squares fits according to equation IV.6.

TABLE I
LEAST-SQUARES FIT TO $C^{(2)}(t,t_0)^2$

Results of the two-parameter least-squares fit to the square $C^{(2)}(t,t_0)^2$ of the two-point time correlation function equation (IV.5), which yields c_0 and $2m$, and to the eigenvalues $\lambda_n(t,t_0)$ of the truncated reduced four-point correlation matrix equation (IV.6) in four sectors, which yields the other values. See also figures IV.6 through IV.10 and section IV.5 of the text.

Note 1. W_6 and c_6 in the A_1 sector have not been included because the error bars on the $n=6$ data were too large.

Note 2. There are no results for the E-sector because all the reduced matrix elements in that sector are identically zero.

Note 3. Notice that the first energy level in the A sector is negative. Although the precision does not allow us any confidence, it is possible that this is a bound state.

Sector	Strength (10^{-16})	Level	Energy	k_n^2
None	c_0 1.916±.049	2m	1.032±.008	0
	c_1 3.614±.103	W_1	1.029±.009	-0.001±.013
A_1	c_2 0.684±.021	W_2	1.098±.010	0.035±.003
	c_3 0.155±.006	W_3	1.180±.013	0.082±.005
	c_4 0.013±.001	W_4	1.372±.034	0.204±.022
	c_5 0.004±.001	W_5	1.415±.073	0.234±.050
	c_1 0.004±.001	W_1	1.497±.060	0.294±.046
A_2	c_1 0.760±.023	W_1	1.115±.009	0.044±.002
	c_2 0.012±.001	W_2	1.381±.035	0.210±.024
	c_3 0.004±.001	W_3	1.354±.079	0.192±.052
B_1	c_1 0.171±.006	W_1	1.209±.012	0.099±.005
	c_2 0.003±.001	W_2	1.522±.071	0.313±.054
	c_3 0±.001	W_3	1.416±.440	0.235±.314

V. SOLUTIONS TO THE SCHRÖDINGER EQUATION

1. Lüscher's Model in Two Space Dimensions

The stationary Schrödinger equation in polar coordinates for two dimensions is

$$-\frac{1}{2m} \left[\frac{1}{r} \frac{\partial}{\partial r} \left(r \frac{\partial}{\partial r} \right) + \frac{1}{r^2} \frac{\partial^2}{\partial \varphi^2} \right] \Psi + V(r) \Psi = E \Psi \quad (\text{V.1})$$

This is solved by the usual separation of variables technique.

The solution of the azimuthal equation is¹

$$Y_{lm}(\varphi) = \frac{1}{\sqrt{2\pi}} e^{il\varphi} \quad \text{where } l \in \mathbb{Z} \quad (\text{V.2})$$

We will write these "circular harmonics" in such a way that they resemble the usual three-dimensional spherical harmonics.

$$Y_{lm}(\varphi) = \frac{1}{\sqrt{2\pi}} e^{im\varphi} \quad \text{where } \begin{array}{l} l \in \mathbb{Z}^+ \text{ and } m = \pm 1 \\ l = 0 \text{ and } m = 0 \end{array} \quad (\text{V.3})$$

The radial solution satisfies the radial Schrödinger equation

$$\left[r^2 \frac{d^2}{dr^2} + r \frac{d}{dr} + (k^2 r^2 - l^2) - 2mr^2 V(r) \right] u(r, k) = 0 \quad (\text{V.4})$$

and is uniquely defined by the normalization condition

$$\lim_{r \rightarrow 0} r^{-l} u'(r, k) = 1$$

Outside the interaction region, where $V(r) = 0$, the regular solution is simply

$$u_l(r,k) = \alpha_l(k)J_l(kr) + \beta_l(k)N_l(kr) \quad (\text{V.5})$$

where $J_l(kr)$ and $N_l(kr)$ are Bessel functions.

The ratio of the Jost coefficients $\alpha \pm i\beta$ is related to the scattering phase shifts δ^2 ,

$$\frac{\alpha_l(k) - i\beta_l(k)}{\alpha_l(k) + i\beta_l(k)} = e^{2i\delta_l(k)} \quad (\text{V.6})$$

a result which is used in the derivation of the determinant equation I.4 for the phase shifts,

$$\det\left(e^{2i\delta(k)} - \frac{M-i}{M+i}\right) = 0$$

This procedure is described in Chapter VI.

2. Singular Periodic Solutions

If we enclose our particles in a planar box of size $L \times L$ and impose periodic boundary conditions, we are giving rise to a periodic potential

$$V_L(\vec{r}) = \sum_{\vec{n} \in \mathbb{Z}^2} V(|\vec{r} + \vec{n}L|) \quad (\text{V.7})$$

$$\Omega = \{\vec{r} \in \mathbb{R}^2 \mid |\vec{r} + \vec{n}L| > R \text{ for all } \vec{n} \in \mathbb{Z}^2\} \quad (\text{V.8})$$

which is not rotationally invariant. Since we have in mind a finite-range potential with some range $R < L/2$, we define an exterior region Ω .

Since $V_L(\vec{r}) = 0$ for $\vec{r} \in \Omega$, a solution of the Schrödinger equation with the potential

V.7 is essentially free in the region Ω . Therefore, its extension to Ω can be matched to some periodic wave that has the asymptotic form V.5 everywhere in each $L \times L$ box except at, at most, isolated points $\vec{r} = \vec{n}L$. Almost all of those periodic waves are singular.

We call a function ψ a singular periodic solution to the Helmholtz equation if

- $\psi(\vec{r})$ is a smooth function defined for all $\vec{r} \neq \vec{n}L$ which satisfies the Helmholtz

equation

$$(\Delta + k^2)\psi(\vec{r}) = 0 \quad \text{with} \quad \Delta = \frac{1}{r} \frac{\partial}{\partial r} r \frac{\partial}{\partial r} + \frac{1}{r^2} \frac{\partial^2}{\partial \phi^2} \quad (\text{V.9})$$

- $\psi(\vec{r})$ is periodic

$$\psi(\vec{r}) = \psi(\vec{r} + \vec{n}L) \quad \text{for all } \vec{n} \in \mathbb{Z}^2 \quad (\text{V.10})$$

- $\psi(\vec{r})$ is bounded by a power of $1/r$

$$\sup_{0 < r < L/2} |r^{\Lambda+1} \psi(\vec{r})| < \infty \quad (\text{V.11})$$

for some whole number Λ . The smallest Λ which satisfies this condition is called the degree of ψ .

The singular periodic solutions play a central role in obtaining phase shifts. It is necessary to construct all of them in practical calculations.³

Towards this goal, we define the Green's function

$$G(\vec{r}, k^2) \equiv L^{-2} \sum_{\vec{p} \in \Gamma} \frac{e^{i\vec{p}\vec{r}}}{p^2 - k^2} \quad (\text{V.12})$$

where Γ is the set of allowable lattice momenta defined by equation III.24. In the definition V.12 we exclude singular values by assuming that $k^2 \neq p^2$ for all $\vec{p} \in \Gamma$.

We can show that

$$(\Delta + k^2)G(\vec{r}, k^2) = - \sum_{\vec{n} \in Z^2} \delta(\vec{r} - \vec{n}L) \quad (\text{V.13})$$

and since G is bounded by a power of $1/r$, it is a singular periodic solution. All other solutions can be constructed from G by using the harmonic polynomials in two dimensions⁴

$$y_{lm}(\vec{r}) = r^l Y_{lm}(\phi) = \frac{1}{\sqrt{2\pi}} (x + imy)^l \quad (\text{V.14})$$

to generate the solutions

$$G_{lm}(\vec{r}, k^2) = y_{lm}(\nabla) G(\vec{r}, k^2) \quad (\text{V.15})$$

These solutions are then used to obtain the elements of the M-matrix. This procedure is described in Chapter VI.

3. Notes

This procedure, including a derivation of the phase shift condition, is explained in more detail in Lüscher (1991a), Lüscher (1991b) and Fiebig, Woloshyn and Domínguez

(1994). Fetter & Walecka (1980) provided the background on solving the Helmholtz equation. The Bessel functions, as needed in this paper, are discussed in Jackson (1975) and Fetter & Walecka (1980). Abramowitz & Stegun (1964) and Gradshteyn & Ryzhik (1980) provided the formulas needed. Watson (1952) provides a wealth of information on Bessel functions and their properties. Schiff (1968) provides a discussion of Levinson's Theorem, which is of relevance to the phase shifts if the first energy level in the A_1 sector (see Table I) is indeed a bound state.

1. Fetter and Walecka (1980), page 279.
2. Taylor (1983), chapter 11.
3. Fiebig, Woloshyn and Dominguez (1994).
4. Fiebig, Woloshyn and Domínguez (1994).

VI. EXTRACTION OF THE PHASE SHIFTS

1. Partial Wave Analysis

The square symmetry group, $O(2,Z)$, has eight elements in five equivalence classes. Thus, it has five irreducible representations¹, which we denote by A_1 , A_2 , B_1 , B_2 and E . As mentioned before, the first four of these are one-dimensional, and the last is two-dimensional.

For fixed l , the harmonic polynomials in two dimensions form representations of $O(2,Z)$.

$$y_{lm}(g^{-1}\vec{r}) = \sum_{m'} y_{lm}(\vec{r}) D_{m'm}^{(l)}(g) \quad \text{for } g \in O(2,Z) \quad (\text{VI.1})$$

with the representation matrices $D^{(l)}(g)$ in equation VI.1 known.²

We can use the explicit form of the $D^{(l)}(g)$ and the group character table to work out the decomposition of each of these angular momentum representations \underline{l} in terms of the irreducible representations of $O(2,Z)$. For the first few values of l , these decompositions of the representations \underline{l} are

$$\underline{0} = A_1$$

$$\underline{1} = E$$

$$\underline{2} = B_1 \oplus B_2$$

$$\underline{3} = E^*$$

$$\underline{4} = A_1 \oplus A_2$$

We are now led to define the following angular functions.

For $l=0$,

$$\psi^{(A_1;0)}(\phi) = Y_{00} = \frac{1}{\sqrt{2\pi}}$$

For $l=4,8,\dots$,

$$\psi^{(A_1;l)}(\phi) = \frac{1}{\sqrt{\pi}} \cos(l\phi)$$

$$\psi^{(A_2;l)}(\phi) = \frac{-1}{\sqrt{\pi}} \sin(l\phi)$$

For $l=2,6,\dots$,

$$\psi^{(B_1;l)}(\phi) = \frac{1}{\sqrt{\pi}} \cos(l\phi)$$

$$\psi^{(B_2;l)}(\phi) = \frac{-i}{\sqrt{\pi}} \sin(l\phi)$$

For $l=1,3,5,\dots$,

$$\psi_{\pm 1}^{(E;l)}(\phi) = \frac{(\pm 1)^{(l+1)/2}}{\sqrt{2}} [Y_{l-1}(\phi) \pm Y_{l+1}(\phi)]$$

2. The Phase Shift Condition

We now define the zeta function ζ arising from our Green's function V.12.

$$\zeta_{lm}(s; q^2) = \sum_{\vec{n} \in \mathbb{Z}^2} Y_{lm}(\vec{n}) (n^2 - q^2)^{-s} \quad (\text{VI.2})$$

Using the transformation property VI.1 of the harmonic polynomials and this definition, we can show (using Schur's Lemma of group theory) that³

$$\sum_m \zeta_{lm}(s; q^2) D_{m/m}^{(l)}(g) = \zeta_{lm}(s; q^2) \quad \text{for all } g \in O(2, Z) \quad (\text{VI.3})$$

Using the explicit form of the $D_{mm}^{(l)}$ again, we discover that $\zeta_{lm}(s; q^2) = 0$ unless $l=0, 4, 8, \dots, \Lambda$, where Λ is some (large) angular momentum cutoff introduced for practical reasons. We also discover that $\zeta_{lm}(s; q^2) = \zeta_{l,-m}(s; q^2)$, which shows that $\zeta_{lm}(s; q^2)$ is real and independent of the value of m . So, hereafter, we will write $\zeta_{lm}(s; q^2)$ simply as $\zeta_l(s; q^2)$.

Now we define the function

$$W_l = -\left(\frac{2}{\pi}\right)^{3/2} \frac{1}{q^l} \zeta_l(1; q^2) \quad \text{with } q = \frac{kl}{2\pi} \quad (\text{VI.4})$$

in terms of which we can calculate all the reduced matrix elements $M_{ll'}$ in all five sectors. (Some formulas for the calculation of $\zeta_l(1; q^2)$ are given in appendix B.)

A₁ Sector

$$M_{00}^{(A_1)} = W_0$$

$$M_{0l}^{(A_1)} = M_{l0}^{(A_1)} = \sqrt{2} W_l \quad \text{for } l=4, 8, \dots, \Lambda$$

$$M_{ll'}^{(A_1)} = W_{|l-l'|} - W_{l+l'} \quad \text{for } l, l'=4, 8, \dots, \Lambda$$

A₂ Sector

$$M_{ll'}^{(A_2)} = W_{|l-l'|} - W_{l+l'} \text{ for } l, l' = 4, 8, \dots, \Lambda$$

B₁ Sector

$$M_{ll'}^{(B_1)} = W_{|l-l'|} + W_{l+l'} \text{ for } l, l' = 2, 6, \dots, \Lambda$$

B₂ Sector

$$M_{ll'}^{(B_2)} = W_{|l-l'|} - W_{l+l'} \text{ for } l, l' = 2, 6, \dots, \Lambda$$

E-Sector

$$M_{ll'}^{(E)} = W_{|l-l'|} \text{ if } |l-l'| = 0 \pmod{4}$$

$$M_{ll'}^{(E)} = -W_{l+l'} \text{ if } |l-l'| = 2 \pmod{4}$$

for $l, l' = 1, 3, \dots, \Lambda$.

The matrix elements in E all turn out to be identically zero because the 2-dimensional representation E is ruled out by the physical symmetries of our system.⁴

We note that the basis transformation to the angular functions of section VI.1 leaves the matrix $e^{2i\delta}$ diagonal since only linear combinations of $Y_{lm}(\phi)$ with different $m = \pm 1$ values are taken. This allows us to separate $e^{2i\delta}$ by representation, and we obtain the determinant condition I.4 also separated by representation,

$$\det[e^{2i\delta^{(\Gamma)}} - U^{(\Gamma)}] = 0 \text{ with } U^{(\Gamma)} = (M^{(\Gamma)} + i)^{-1}(M^{(\Gamma)} - i) \quad (\text{VI.5})$$

The phase shifts $\delta_1^{(\Gamma)}(k_n^2)$ for the four representations A_1 , A_2 , B_1 , and B_2 , can now be obtained numerically. The results are given in table II. The angular momentum cutoff was chosen as $\Lambda=8$. Some of these $\delta_1^{(\Gamma)}(k_n^2)$ from table II were then plotted versus their corresponding relative momentum squared (which can be found in table I). The resulting graphs are shown in figures VI.1 through VI.3. In the graphs, some of the points have been relocated modulo 180° because the phase shift condition I.4 only determines the phase shifts modulo π .

3. Notes

Hammermesh (1962) provides all the background material on group theory, including discussions on Schur's Lemma and the square symmetry group. Taylor (1983) and Schiff (1968) provide all the background material on scattering theory, including discussions of phase shifts and their interpretations. Lüscher (1991a), Lüscher (1991b) and Fiebig, Woloshyn and Domínguez (1994) discuss both the derivation of the determinant condition I.4 on the phase shifts and the calculation of the reduced elements of the M-matrix..

1. Hammermesh (1962), chapter 7.
2. Hammermesh (1962), chapter 7.
3. Hammermesh (1962), chapter 7.
4. Fiebig, Woloshyn and Domínguez (1994).

TABLE II
PHASE SHIFTS $\delta_1^{(\Gamma)}(k_n^2)$

The phase shifts $\delta_1^{(\Gamma)}(k_n^2)$ in degrees for the five representations Γ and their particular dominant partial waves l (with their corresponding errors) for different energy levels. Recall that the phase shift condition I.4 only determines the phase shifts modulo π (or 180°).

Γ	l	$n=2$	$n=3$	$n=4$	$n=5$
A_1	0	50.5(8.1)	-16.7(7.9)	64.5(41.8)	28.3(37.9)
A_1	4	1.1(0.2)	-23.1(26.4)	-68.6(57.4)	35.2(80.4)
A_1	8	0.0(0.0)	0.003(0.001)	1.08(0.62)	2.04(1.54)

Γ	l	$n=1$	$n=2$	$n=3$
A_2	4	14.7(15.9)		
A_2	8	-7.6(7.8)		
B_1	2	12.9(1.3)	34.5(18.7)	51.8(58.3)
B_1	6	0.022(0.007)	12.2(0.8)	12.0(2.4)
B_2	2	23.8(3.9)	12.5(25.3)	88.0(368.0)
B_2	6	-1.3(0.3)	-88.5(143.0)	-20.7(165.0)

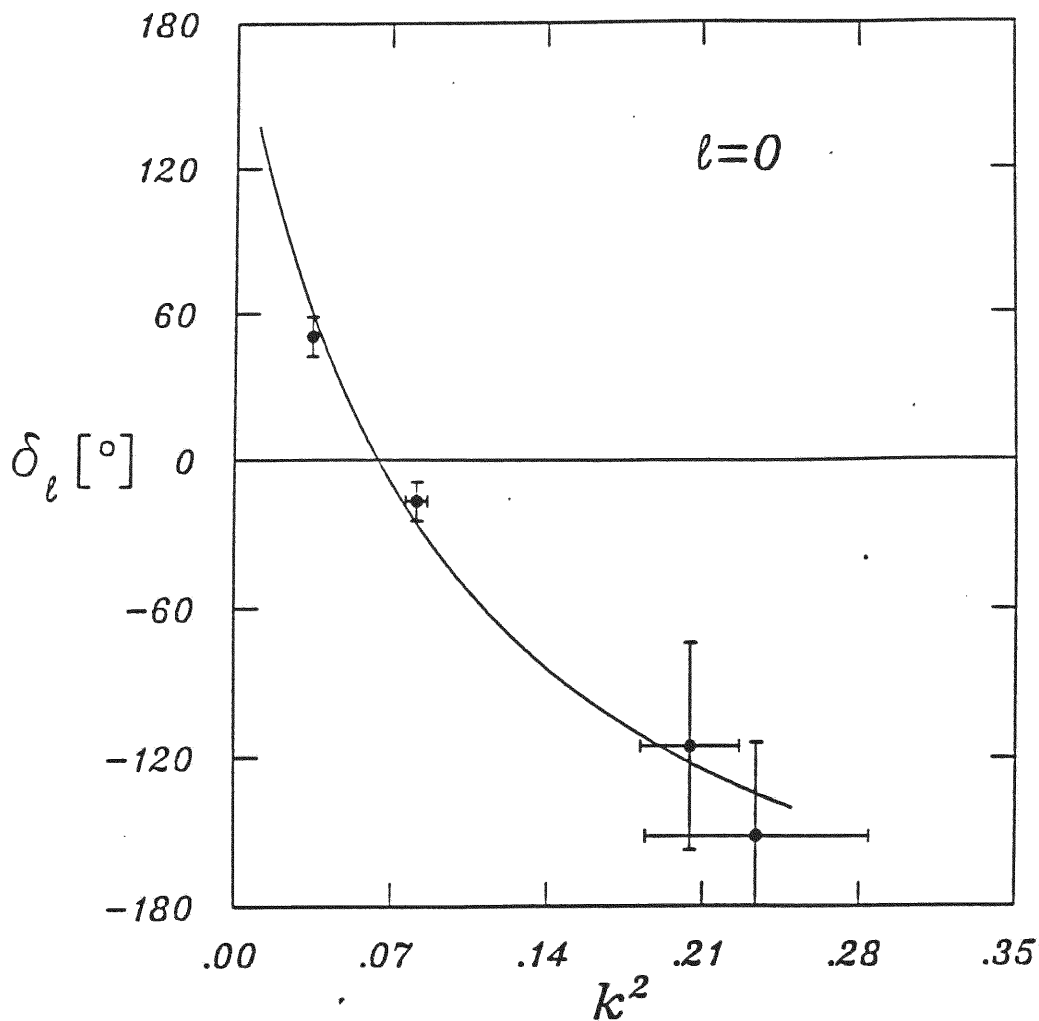


FIGURE VI.1
PHASE SHIFTS FOR PARTIAL WAVE $l=0$

This graph shows the phase shift in degrees for the partial wave $l=0$ versus the relative momentum squared. The data are from the A_1 sector. See Table II for a tabulation of the numerical results and chapters VI and VII for an interpretation of this graph.

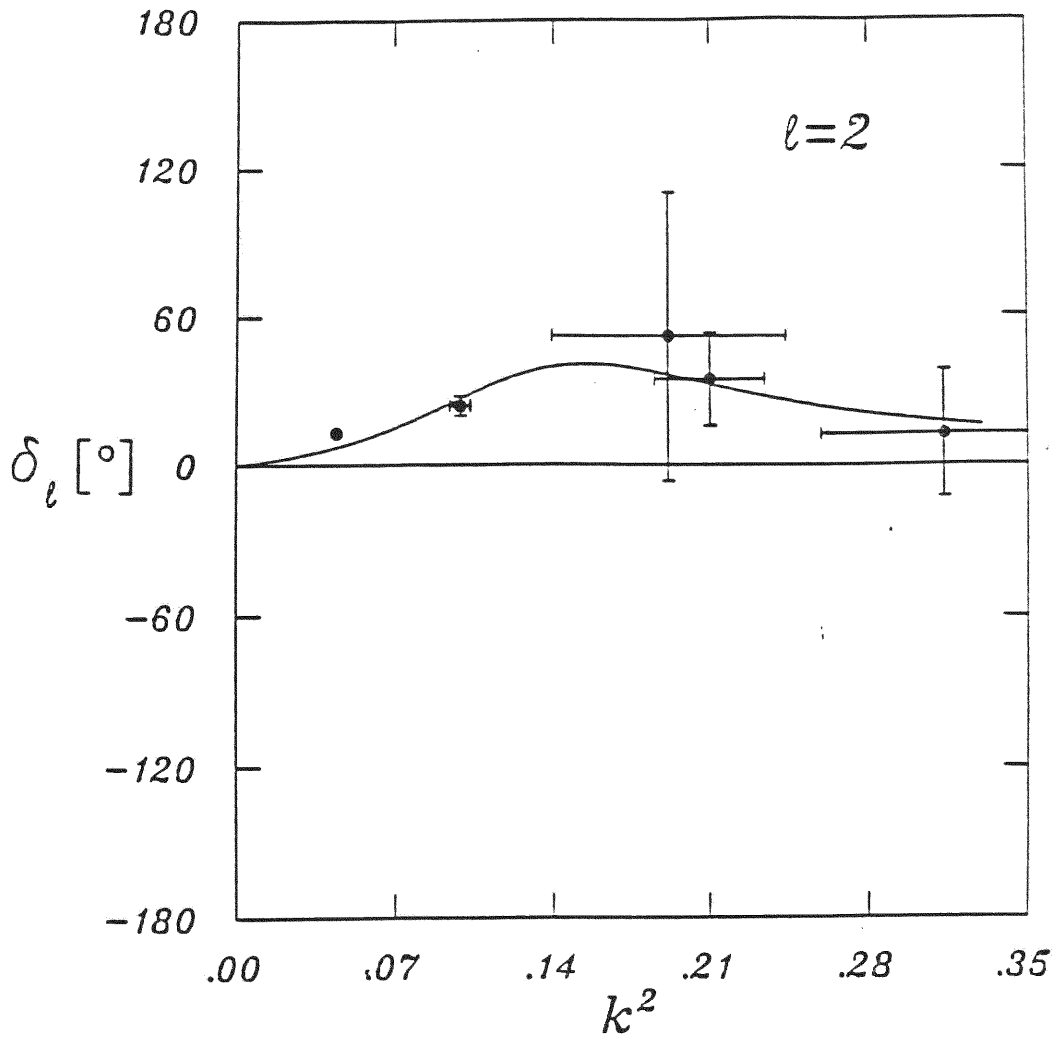


FIGURE VI.2
PHASE SHIFTS FOR PARTIAL WAVE $l=2$

This graph shows the phase shift in degrees for the partial wave $l=2$ versus the relative momentum squared. The data are from the B_1 and B_2 sectors. See Table II for a tabulation of the numerical results and chapters VI and VII for an interpretation of this graph.

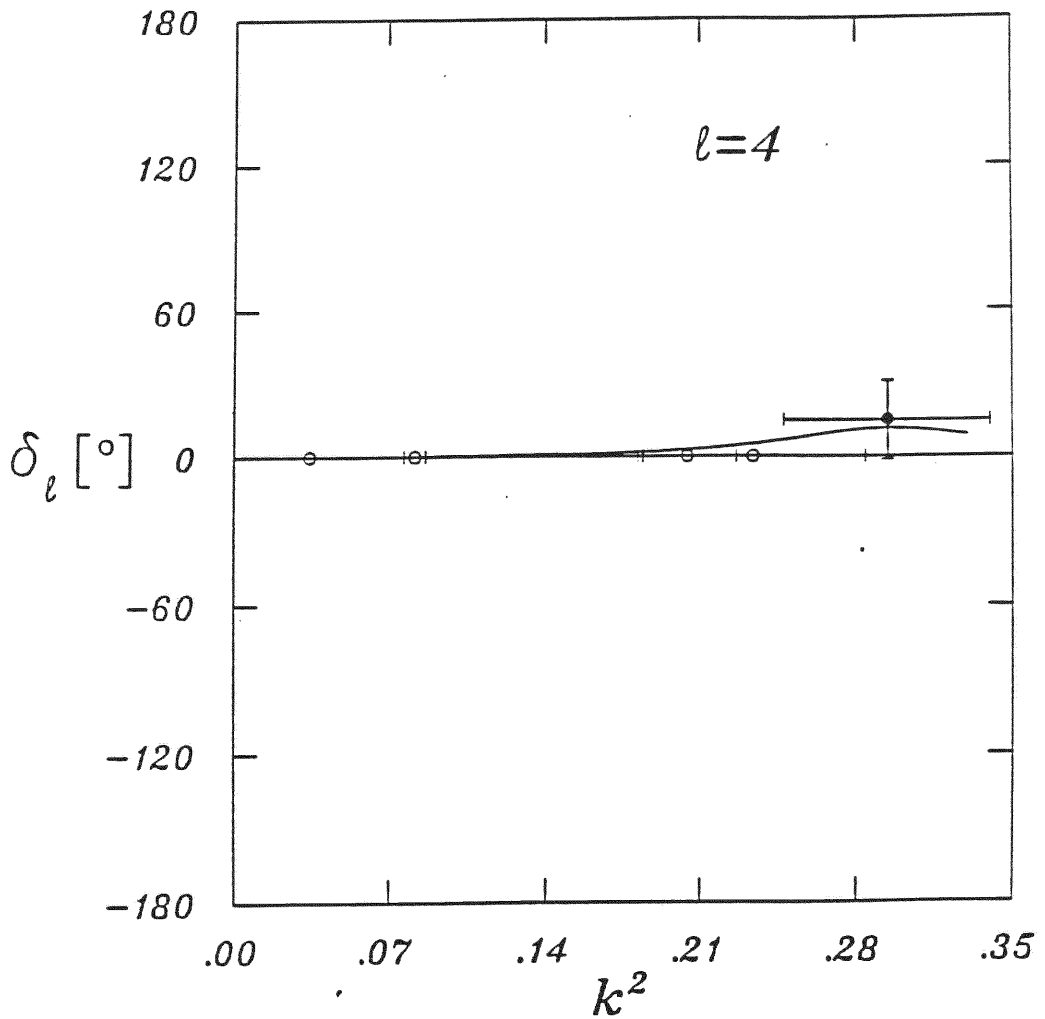


FIGURE VI.3
PHASE SHIFTS FOR PARTIAL WAVE L=4

This graph shows the phase shift in degrees for the partial wave $l=4$ versus the relative momentum squared. The filled plot symbol is from the A_2 sector. See Table II for a tabulation of the numerical results and chapters VI and VII for an interpretation of this graph.

VII. CONCLUSION

1. Explanation of Results

We can not expect equation VI.5 to have a unique solution because in general there are more parameters than determining equations (especially if the angular momentum cutoff Λ is large). We solved the equation by imposing the constraint that for a fixed partial wave l , $\delta_l^{(\Gamma)}=0$ if $l \neq 1$. We furthermore adopted the point of view that the dominant angular momentum is given by the smallest value of l within each sector Γ . Referring to the results given in table II, this means that the s-wave phase shift δ_0 is given by $\delta_0^{(A1)}$, the d-wave phase shift δ_2 is given by $\delta_2^{(B1)}$ and $\delta_2^{(B2)}$, and the g-wave phase shift δ_4 is given by $\delta_4^{(A2)}$. Equation I.4 does not determine the phase shifts exactly. The phase shifts are only determined up to modulo π . This fact was used when plotting the phase shifts in figures VI.1, VI.2 and VI.3.

The data points for δ_0 in figure VI.1 are consistent with a smooth curve which decreases rapidly as k^2 increases. This is reminiscent of the result for classical hard-sphere scattering, and is typical for repulsive interactions. Figures VII.1 and VII.2 show typical scattering waves for the $l=0$ and $l=2$ cases, respectively. If we look at these two figures, we see (1) that the probability amplitude for two mesons being close together is largest in the s-wave and (2) that the probability amplitude in the s-wave is only considerable if the two mesons are close together. This would indicate a near-static (because we only considered small values of the momentum) repulsive interaction at small distances, a result reminiscent of the Pauli exclusion principle.

In figure VI.2, the data suggest positive phase shifts over a broad k^2 interval. This is consistent with an attractive interaction. If we again look at figures VII.1 and VII.2, we see (1) that the probability amplitude for two mesons being at an intermediate distance is largest in the d-wave and (2) that the probability amplitude for two mesons being close together is strongly suppressed in the d-wave. This would indicate a near-static (as before) attractive interaction at intermediate distance.

Despite the simple quenched QED_{2+1} model used, our simulation seems to have the properties one would expect of nuclear physics on a lattice. We have shown that it is possible to calculate scattering phase shifts between composite particles and that the results can be interpreted in a way compatible with reasonable expectations. However, the procedure is complicated and requires a lot of computational effort.

Since the meson fields in our quenched simulation are constructed from fermion-antifermion fields which live on the same site \mathbf{x} , it should be clear that the residual attraction between the mesons is due to the dynamics of the gauge fields. In contrast, in traditional nuclear theory, intermediate-range attraction is due to the exchange of elementary boson fields. The traditional (phenomenological) boson exchange model relies on ω -meson exchange to explain the short-range repulsion, ρ -meson exchange to explain the intermediate-range attraction, and π -meson exchange to explain the long-range residual attraction. It would seem that this new model may be able to provide a much more fundamental explanation of the strong nuclear force.

2. Consideration of Future Work

There are three directions that future research in this field needs to take. First, our interpretation of the phase shifts is in need of better simulations before we are able to draw conclusions with confidence. Second, it would be desirable to obtain a static potential from a lattice simulation, for example, extracted from the two-body energy versus distance. Such a simulation would rely upon the computation of the four-point time correlation matrix and would be feasible with the methods presented here. Third and most difficult, it is necessary to repeat all of this work on scattering phase shifts for QCD_{3+1} , which is the physically meaningful model that is ultimately of concern to us.

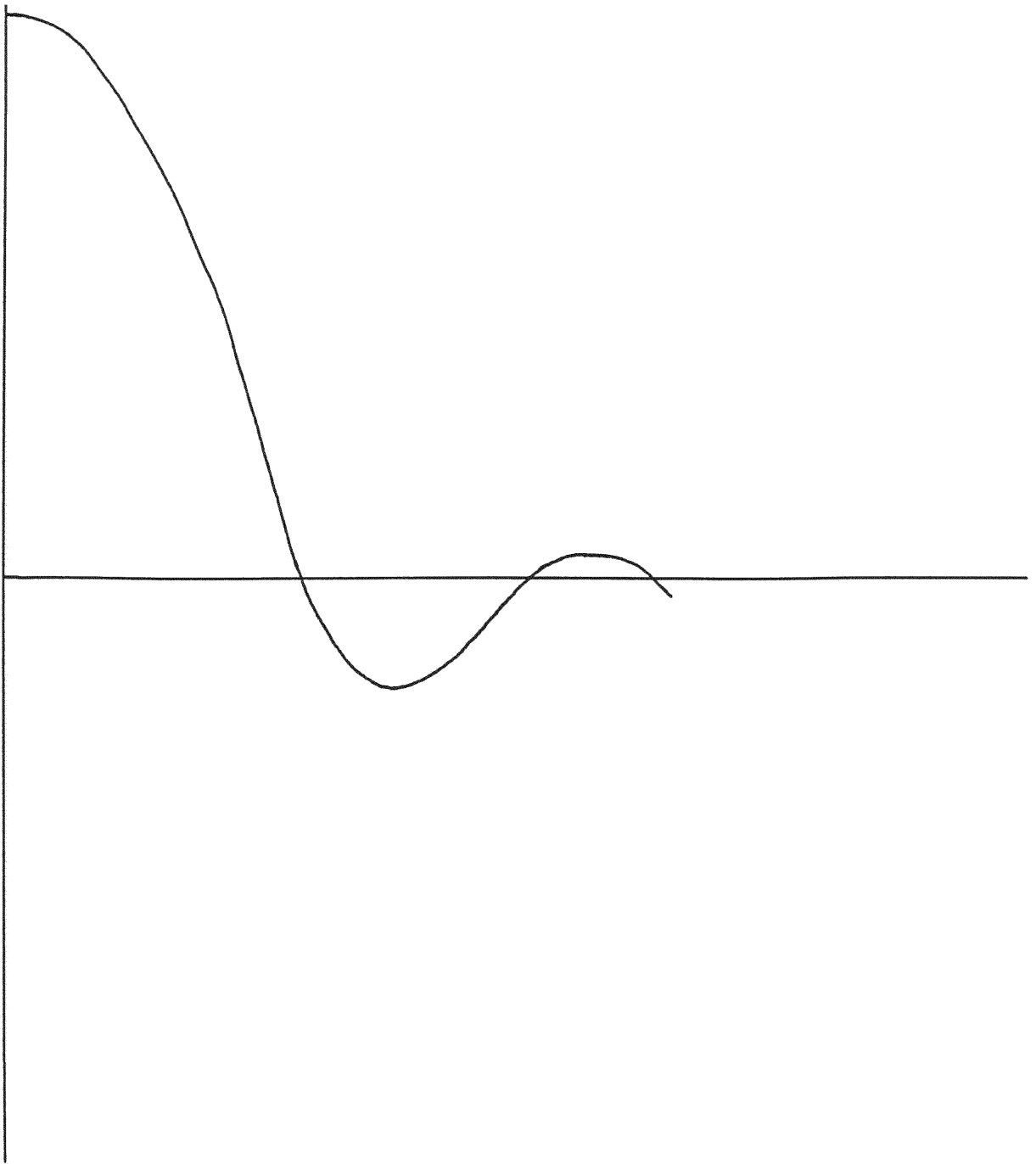


FIGURE VII.1
TYPICAL SCATTERING WAVE FOR $L=0$

A typical scattering s-wave. Note that the probability amplitude is only large if the two mesons are a short distance from each other. The importance of this to our results is discussed in the text in section VII.1.

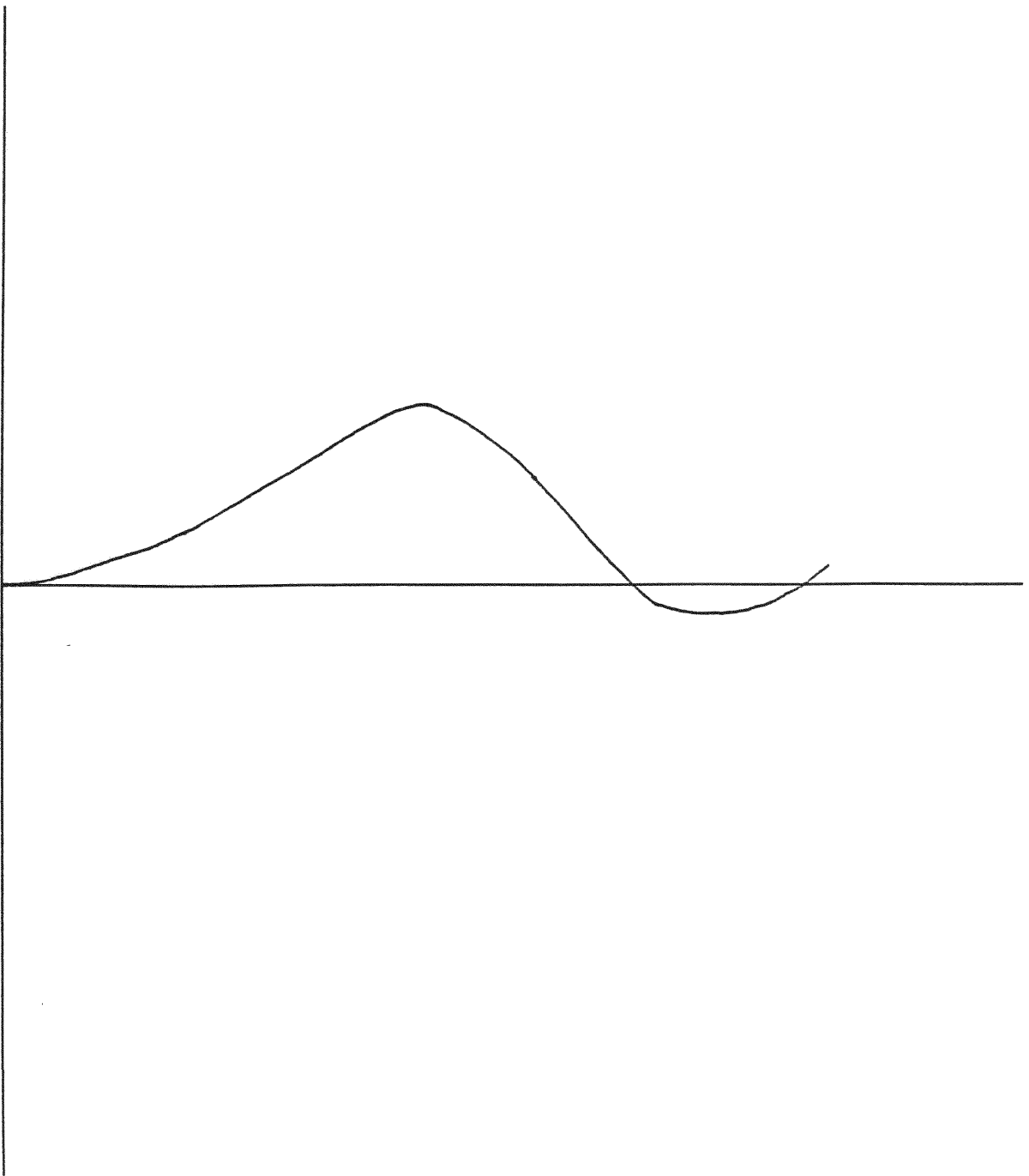


FIGURE VII.2
TYPICAL SCATTERING WAVE FOR $L=2$

A typical scattering d-wave. Note that the probability amplitude is only considerable if the two mesons are at an intermediate distance from each other. The importance of this to our results is discussed in the text in section VII.1.

APPENDIX A

Here we derive formulas for the computation of the zeta functions $\zeta_{\text{lm}}(1; q^2)$ defined by equation VI.2, following the procedure given in Lüscher (1991a). An appendix of Fiebig, Woloshyn and Domínguez (1994) gives a numerically improved procedure for calculating these zeta functions.

We begin by using Green's theorem in 2 dimensions to find that

$$(\Delta + k^2)N_0(kr) = 4\delta(\vec{r}) \quad (\text{A.1})$$

Restricting ourselves to an open neighborhood of $r=0$, we can extract the singularity from the Green's function defined by equation V.12, to obtain

$$G(\vec{r}, k^2) = -\frac{1}{4}N_0(kr) + \hat{G}(\vec{r}, k^2) \quad (\text{A.2})$$

where the remainder is nonsingular.

For convenience we rewrite (A.2) as

$$\hat{G}(\vec{r}, k^2) = L^{-2} \sum_{\vec{p} \in \Gamma} \frac{e^{i\vec{p}\vec{r}}}{p^2 - k^2} + \frac{1}{4}N_0(kr) \quad (\text{A.3})$$

We will take $\vec{p} = \frac{2\pi}{L}\vec{n}$, $\vec{r} = \frac{L}{2\pi}\vec{\rho}$ and $k = 2\pi q/L$. We will also assume

that k^2 is such that $q^2 \neq |\mathbf{n}|^2$ for all $\mathbf{n} \in \mathbb{Z}^2$.

For a fixed value of q^2 , now choose $v \in \mathbb{R}$ such that $v^2 > q^2$. Then (A.3) can be rewritten as

$$\hat{G}(\vec{r}, k^2) = \sum_{|\vec{n}| < v} \frac{(2\pi)^{-2} e^{i\vec{n}\vec{r}}}{n^2 - q^2} + \frac{1}{4} N_0(kr) + \int_0^\infty e^{iq^2 t} K^v(t, \vec{\rho}) \quad (\text{A.4})$$

with the truncated heat kernel

$$K^v(t, \vec{\rho}) = \frac{1}{2\pi} \sum_{|\vec{n}| \geq v} e^{i\vec{n}\vec{r} - tn^2} \quad (\text{A.5})$$

Note that the integrand in (A.4) drops off at least as fast as $e^{-(v^2 - q^2)t}$ for large t. For

small t, we use an alternate untruncated representation of the heat kernel

$$K^0(t, \vec{\rho}) = \sum_{|\vec{n}| > v} \frac{1}{4\pi t} e^{-(\vec{\rho} - 2\pi\vec{n})^2/4t} \quad (\text{A.6})$$

The truncated heat kernel can then be calculated from

$$K^v(t, \vec{\rho}) = K^0(t, \vec{\rho}) - (2\pi)^{-2} \sum_{|\vec{n}| < v} e^{i\vec{n}\vec{r} - tn^2} \quad (\text{A.7})$$

In a neighborhood of $\rho=0$, the integrand in (A.4) is dominated by the $n=0$ term as $t \rightarrow 0$.

$$K^v(t, \vec{\rho}) = \frac{1}{4\pi t} e^{-\rho^2/4t} + \dots \quad (\text{A.8})$$

Thus the integrand of (A.4) can be rewritten

$$\begin{aligned} \int_\infty^0 dt e^{iq^2 t} K^v(t, \rho^2) &= \int_{q^{-2}}^0 dt [e^{iq^2 t} K^v(t, \rho^2) - \frac{1}{4\pi t} e^{-\rho^2/4t}] \\ &+ \int_\infty^{q^{-2}} dt e^{iq^2 t} K^v(t, \rho^2) + \int_{q^{-2}}^0 dt \frac{1}{4\pi t} e^{-\rho^2/4t} \end{aligned} \quad (\text{A.9})$$

The last integral can be expressed in terms of an incomplete gamma function

$$\int_0^q q^{-2} dt \frac{1}{4\pi t} e^{\rho^2/4t} = \frac{1}{4\pi} \Gamma(0, \frac{q^2 \rho^2}{4})$$

$$= -\frac{1}{4\pi} [\ln(q^2 \rho^2) + \gamma + \sum_{m=1}^{\infty} \frac{(q^2 \rho^2)^m}{m! m}]$$

which reveals a logarithmic singularity. The logarithmic singularities contained in $\frac{1}{4}N_0(kr)$ and in this expression cancel out exactly. Expressed in a more formal manner, this means that we have

$$\frac{1}{4}N_0(q\rho) + \int_0^q q^{-2} dt \frac{1}{4\pi t} e^{-\rho^2/4t} = \frac{1}{4\pi} \gamma + \Theta(\rho) \quad (\text{A.10})$$

where $\Theta(\rho)$ is a function of $\rho=|\rho|$ with $\Theta(\rho \rightarrow 0)=0$.

Using (A.4), (A.9) and (A.10), we obtain

$$\hat{G}(\vec{r}, k^2) = \sum_{|\vec{n}| < \nu} \frac{(2\pi)^{-2} e^{i\vec{n}\cdot\vec{\rho}}}{n^2 - q^2}$$

$$+ \int_0^q q^{-2} dt [e^{iq^2} K^\nu(t, \vec{\rho}) - \frac{1}{4\pi t} e^{-\rho^2/4t}]$$

$$+ \int_q^\infty q^{-2} dt e^{iq^2} K^\nu(t, \vec{\rho}) + \frac{1}{4\pi} \gamma + \Theta(\rho) \quad (\text{A.11})$$

Having removed the singularity, the above function is now regular at $r=0$. We may thus expand

$$\hat{G}(\vec{r}, k^2) = \sum_{lm} \hat{g}_{lm} J_l(kr) Y_{lm}(\Phi) \quad (\text{A.12})$$

The coefficients are given by

$$\hat{g}_{lm} = \lim_{r \rightarrow 0} l! \left(\frac{kr}{2}\right)^{-l} \int_0^{2\pi} d\phi Y_{lm}^*(\phi) \hat{G}(\vec{r}; k^2) \quad (\text{A.13})$$

Using the partial wave expansion

$$e^{i\vec{p}\cdot\vec{r}} = \sum_{lm} 2\pi i^l J_l(pr) Y_{lm}(\phi) Y_{lm}^*(\phi) \quad (\text{A.14})$$

we obtain the relation

$$\hat{g}_{lm} = \frac{i^l}{2\pi q^l} \zeta_{lm}(1; q^2) \quad (\text{A.15})$$

with the zeta function now given by

$$\begin{aligned} \zeta_{lm}(1; q^2) &= \sum_{|\vec{n}| < q} y_{lm}(\vec{n}) (n^2 - q^2)^{-1} \\ &+ \int_0^{q^{-2}} dt [e^{iq^2} K_{lm}^{\vee}(t) - \delta_{l0} \sqrt{\frac{\pi}{2}} \frac{1}{t}] \\ &+ \int_{q^{-2}}^{\infty} dt e^{iq^2} K_{lm}^{\vee}(t) + \delta_{l0} \sqrt{\frac{\pi}{2}} \gamma \end{aligned} \quad (\text{A.16})$$

The functions $K_{lm}^\nu(t)$ can be computed by

$$K_{lm}^\nu(t) = \sum_{|\vec{n}| \geq \nu} Y_{lm}(\vec{n}) e^{-t n^2} \quad (\text{A.17})$$

$$= (-i)^l \left(\frac{\pi}{l}\right)^{l+1} \sum_{\vec{n} \in \mathbb{Z}^2} Y_{lm}(\vec{n}) e^{-\pi^2 n^2 / t} - \sum_{|\vec{n}| < \nu} Y_{lm}(\vec{n}) e^{-t n^2} \quad (\text{A.18})$$

where (A.17) is suitable for large t , and (A.18) is suitable for small t .

APPENDIX B

Here we describe the most essential features of the square symmetry group $O(2,Z)$.

For each n in Z define the complex number $n = n + in$ in C . The action of the eight elements of $O(2,Z)$ on the vector n is then given by

$$\begin{array}{cccc}
 E n = n & R n = i n & R^2 n = -n & R^3 n = -i n \\
 P_1 n = n^* & P_2 n = -n^* & Q_1 n = i n^* & Q_2 n = -i n^*
 \end{array}$$

where R is the rotation by 90° , P_1 and P_2 are rotations about the real and imaginary axis, respectively, and Q_1 and Q_2 are reflections about the two diagonal axis in the complex n plane. The inversion (or parity) operator, $I n = -n$, is identical to R^2 .

The eight elements of $O(2,Z)$ fall into eight equivalence classes. These classes are

$$\begin{array}{l}
 C_1 = \{ E \} \quad C_2 = \{ R \} \quad C_3 = \{ R, R^3 \} \\
 C_4 = \{ P_1, P_2 \} \quad C_5 = \{ Q_1, Q_2 \}
 \end{array}$$

Group theory tells us that for any group the number of irreducible representations equals the number of equivalence classes. Thus, there are five irreducible representations of $O(2,Z)$, four of which are one-dimensional (these are traditionally named A_1 , A_2 , B_1 and B_2) and one of which is two-dimensional (which is traditionally named E). These irreducible representations are most conveniently expressed in terms of basis functions which are polynomials in n and n^* .

$$\psi^{(A1)}(n) = n^* n$$

$$\psi^{(B)}(n) = \text{Im } n$$

$$\psi^{(B1)}(n) = n^2 + n^{*2}$$

$$\psi^{(B2)}(n) = n^2 - n^{*2}$$

$$\psi_1^{(E)}(n) = n \quad \psi_2^{(E)}(n) = n^*$$

We now concern ourselves with finding the transformation properties of the harmonic polynomials in two dimensions.

Using equation (VI.1) we obtain

$$D_k(R) = \delta_{k,i} \quad \text{for } k = 0, 1, 2, 3$$

$$D_k(P) = \delta_{k,0} \quad D_k(P) = \delta_{k,-1}$$

$$D_{m'm}^{(0)}(Q_1) = \delta_{m,-m}(im')^l \quad D_{m'm}^{(0)}(Q_2) = \delta_{m,-m}(-im')^l$$

More reference material on group theory, in general, and the square symmetry group, in particular, can be found in Hammermesh (1962).

LIST OF REFERENCES

- M. Abramowitz and I. Stegun (1964). *Handbook of Mathematical Functions*, Dover, New York.
- I. J. R. Aitchison and A. J. R. Hey (1989). *Gauge Theories in Particle Physics, Second Edition*, IOP Publishing, Bristol.
- T. Appelquist, M. Bowick, E. Cohler and L. Wijewardhana (1985). *Physical Review Letters* 55, 1715.
- I. M. Barbour and C. J. Burden (1985). *Physics Letters B* 161, 357.
- ____ P. Gibbs, K. Bowler and D. Roweth (1985). *Physics Letters B* 158, 61.
- ____ J. Gilchrist, H. Schneider, G. Schierholtz and M. Teper (1984). *Physics Letters B* 136, 80.
- F. S. Beckman (1960), in *Mathematical Methods for Digital Computers*, edited by A. Ralston and H. Wilf, Wiley, New York.
- R. Bellman (1970). *Introduction to Matrix Analysis, Second Edition*, McGraw-Hill, New York.
- C. J. Burden and A. N. Burkitt (1987). *Europhysics Letters* 3, 545.
- T.-P. Cheng and L.-F. Li (1984). *Gauge Theories of Elementary Particle Physics*, Oxford University Press, New York.
- P. D. Coddington, A. J. R. Hey, A. A. Middleton and J. S. Townsend (1986). *Physics Letters B* 175, 64.
- N. G. Cooper and G. B. West, editors (1988). *Particle Physics: A Los Alamos Primer*, Cambridge University Press, Cambridge.
- M. Creutz (1983). *Quarks, Gluons and Lattices*, Cambridge University Press, Cambridge.
- E. Dagotto, J. B. Kogut and A. Kocic (1989). *Physical Review Letters* 62, 1083.
- B. Efron (1979). *SIAM Review* 21, 460.
- A. L. Fetter and J. D. Walecka (1971). *Quantum Theory of Many-Particle Systems*, McGraw-Hill, New York.

- _____ (1980). *Theoretical Mechanics of Particles and Continua*, McGraw-Hill, New York.
- H.R. Fiebig and R. M. Woloshyn (1990). *Physical Review D* 42, 3520.
- _____ (1991). *Nuclear Physics B (Proceedings Supplements)* 20, 655.
- _____ and A. L. Domínguez (1994). *Nuclear Physics B* 418, 637.
- D. Fries and B. Zeitnitz, editors (1982). *Quarks and Nuclear Forces*, Springer Tracts in Modern Physics, Volume 100, Springer-Verlag, Berlin.
- S. Gottlieb, W. Liu, D. Toussaint, R. Renken and R. Sugar (1987). *Physical Review D* 35, 2531.
- I. S. Gradshteyn and I. M. Ryzhik (1980). *Table of Integrals, Series and Products*, Academic Press, San Diego.
- M. Guagnelli, E. Marinari and G. Parisi (1990). *Physics Letters B* 240, 188.
- H. Hamber, E. Marinari, G. Parisi and C. Rebbi (1983). *Nuclear Physics B* 225, 475.
- M. Hammermesh (1964). *Group Theory and its Application to Physical Problems*, Addison-Wesley, Reading.
- I. S. Hughes (1985). *Elementary Particles, Second Edition*, Cambridge University Press, Cambridge.
- A. Ivic (1985). *The Riemann Zeta Function*, Wiley, New York.
- J. D. Jackson (1975). *Classical Electrodynamics, Second Edition*, Wiley, New York.
- N. Kawamoto and J. Smit (1981). *Nuclear Physics B* 192, 100.
- H. Kluberg-Stern, A. Morel, O. Napoly and B. Petersson (1983). *Nuclear Physics B* 220 [FS8], 447.
- J. B. Kogut (1979). *Reviews of Modern Physics* 51, 659.
- _____ and L. Susskind (1975). *Physical Review D* 11, 395.
- M. Lüscher (1986). *Comm. Math. Phys.* 105, 153.
- _____ (1991a). *Nuclear Physics B* 354, 531.